Contribution of neurons in monkey parietal cortex to a visual grouping

Isao Yokoi

DOCTOR OF PHYLOSOPHY

Department of Physiological Sciences

School of Life Science

The Graduate University for Advanced Studies

2010

Table of Contents

Abstract

Visual grouping is an essential component of the visual perception of objects. It is the process by which multiple discrete elements are bound into a single object. Visual grouping is caused by bottom-up factors such as similarity and continuity of the dots. It is also known that visual grouping is affected by top-down factors such as prior knowledge and past experience with the objects. Neurological observations made in human patients and in fMRI studies of healthy human subjects suggest that the posterior parietal cortex plays a key role in visual grouping. It remains unknown, however, how parietal cortex are involved in visual grouping.

To investigate the neuronal mechanisms underlying visual grouping, we designed a grouping detection task controlled by top-down attention, and performed extra-cellular single unit recording from lateral bank of intra-parietal sulcus (L-IPS) while the task was being performed by monkeys. The visual stimuli consisted of multiple discrete dots, and the monkeys were required to detect the target defined by specific arrangements of the dots. In addition, we manipulated the monkeys' attention to the grouping of the elements, and examined the effect of attention on the neuronal responses. The visual stimuli were composed of 5 square black or white dots (1.2 deg at the edge) arranged in a cross. A total of 20 types of visual stimuli composed of different arrangements of dots were prepared. In four of the 20 stimuli, three dots with the same contrast (either black or white) were aligned either horizontally or vertically and these four stimuli served as the target. The remaining 16 stimuli were non-targets. The target stimuli were characterized by two visual features: the orientation of the three dots with the same contrast that was either horizontal or vertical (target orientation) and the contrast of three-aligned dots, which was either white or black (target contrast). The monkeys performed the detection

task while their attention was directed towards a particular target orientation.

We recorded the activities of 107 single neurons in the L-IPS while two monkeys performed a grouping detection task. We found that L-IPS neurons selectively responded to the visual stimulus, and a majority of neurons exhibited stronger selectivity for the target orientation than the target contrast. This orientation selectivity was enhanced when the target orientation matched the attended orientation. Moreover, the orientation-selective responses correlated with the monkeys' behavior. These results suggest that L-IPS neurons play important roles in the visual grouping and detection of objects comprised of discrete elements.

Although it is known that there are two functional classes of cortical neurons, excitatory pyramidal neurons and inhibitory interneurons, it remains largely unknown how these two classes contribute to visual perception and cognition. Recently, several attempts have been made to classify extracellularly recorded neurons according to known differences in the waveforms of their action potentials (e.g., Mitchell et al., 2007, Neuron). These studies suggest that classification of neuron type will provide valuable new information that could be crucial to understanding neural processing within local circuits in the cerebral cortex.

In order to examine how different classes of neurons are involved in visual grouping, we classified recorded neurons according to the waveforms of their action potentials, and compared the response properties of classified neurons. We found that putative pyramidal neurons, which had broader action potentials, exhibited selectivity for the target orientation, and the selectivity was enhanced by attention. By contrast, putative inhibitory neurons, which had narrower action potentials, did not exhibit such selectivity or enhancement. Instead interneurons responded more strongly to the target stimuli

than to the non-targets, regardless of the orientation of the target. These results suggest that different classes of parietal neurons contribute differently to the visual grouping of discrete elements.

Classification of L-IPS neurons showed that pyramidal neurons exhibited selectivity for the target stimulus, and clearly indicates that L-IPS neurons signal information about the grouped stimulus to other cortical areas. Neurons in L-IPS may provide feedback signals and affect the activity related to visual grouping in the early visual area. However, no study has explored in detail the feedback projection related to the visual grouping. In an attempt to study the contribution of feedback projection on visual grouping, we examined whether there is an anatomical basis for integration of visual signals from both sides of blind spot (BS) by cortico-geniculate feedback neurons in V1. The blind spot is the region in the visual field that corresponds to the optic disk in the retina. No visual information exists in the blind spot because there is no photoreceptor within the optic disk. Nonetheless, we perceive color and/or patterns there that are the same as in the surrounding visual field. This phenomenon is known as perceptual filling-in, and closely related to the visual grouping. Neural mechanisms under perceptual filling-in at the blind spot has been examined in detail, and this provides a good physiological model to investigate the anatomical basis for integration of visual signals related to visual grouping.

We recorded neuronal activity from V1 of a cat and mapped the receptive fields of V1 neurons. After identifying the blind spot region in V1, we inserted a glass micropipette filled with biotinylated dextran amine (BDA) into a location adjacent to the blind spot region in V1, and injected BDA by iontophoresis. BDA labeled axons were traced around the neuron-free gap in layer A of LGN. We observed that numerous

axons traverse the neuron-free gap that retinotopically corresponds to BS within LGN. This indicates that visual signals from one side of BS are conveyed to the opposite side via a feedback connection. Cortico-geniculate feedback projection may integrate visual signals from around BS and contribute to perceptual filling-in at BS.

We recorded neuronal activities in L-IPS while monkeys performed a grouping detection task. We found that pyramidal neurons in L-IPS exhibited selectivity for the orientation of the target, and this selectivity was enhanced by attention to a particular target orientation. This result indicates that L-IPS neurons signal information about the grouped stimulus to other cortical areas. In the anatomical experiment, we found the feedback connection linking the visual fields surrounding the blind spot, which may be involved in the integration or interaction of visual information present at separate locations within the visual field. Neuronal activity in V1 is modulated by the presentation of visual stimuli in the receptive field surround, and it has been suggested that this contextual modulation is related to the visual grouping (Gilbert et al., 2000). Presumably, L-IPS neurons provide feedback signals to the early visual areas and facilitate visual grouping by way of the contextual modulation there.

These results provide the first physiological evidence that L-IPS neurons make an important contribution to visual grouping by combining visual and attentional signals to bind discrete visual elements. A recurrent circuit between the L-IPS and early visual areas may be critical for visual grouping through the interchange of feedforward and feedback signals.

General introduction

Visual grouping is an essential component of the visual perception of objects. It is the process by which multiple discrete elements are bound into a single object, and has been extensively studied by Gestalt psychologists. It is known, for example, if multiple dots with the same color are arranged along a straight line, these dots are grouped together and recognized as a single linear object. This grouping is caused by the similarity and continuity of the dots; in other words, the image elements are grouped together based on the relationship among the multiple elements. Visual grouping is also affected by top-down factors, such as prior knowledge, past experience with the objects (Wertheimer 1950; Palmer 1999).

Neurological studies of human patients suggest that the posterior parietal cortex plays a key role in visual grouping. Patients with Balint's syndrome, who have bilateral damage to the parietal cortex, cannot perceive a visual scene as a whole; instead, they see only one of the multiple objects in a visual scene at a time. It has therefore been suggested that the posterior parietal cortex is involved in the integration of multiple objects and features and in global gestalt perception. (Warrington and James, 1967; Coslett and Saffran, 1991; Friedman-Hill et al., 1995; Himmelbach et al., 2009). It has also been reported that patients with unilateral damage to the parietal cortex have an impaired ability to allocate attention to promote visual grouping (Robertson et al., 1988), which suggests that the parietal cortex is also involved in visual grouping controlled by top-down attention. However, it remains unknown how parietal cortex are involved in visual grouping.

Many studies have shown that neurons in the lateral bank of the intra-parietal sulcus (L-IPS) are involved in spatial attention or selection and control of visually guided

eye/hand movements (Gnadt and Andersen, 1988; Taira et al., 1990; Barash et al., 1991; Colby et al., 1996; Snyder et al., 2000; Shadlen and Newsome, 2001; Bisley and Goldberg, 2003, 2006). However, there have been no studies examining the involvement of parietal neurons in visual grouping. We investigate the neuronal mechanism underlying visual grouping in the following three experiments.

In the experiment described in Part 1, we tested how parietal neurons represent the grouping stimulus, and how these activities are affected by the top-down attention. We designed a grouping detection task controlled by top-down attention. The visual stimuli consisted of multiple discrete dots, and the monkeys were required to detect the target defined by specific arrangements of the dots. Visual grouping was necessary for detection of the target. In addition, we manipulated the monkeys' attention to the grouping of the elements. We recorded the activities of single neurons in the L-IPS while two monkeys performed a grouping detection task. We found that L-IPS neurons selectively responded to target stimulus, that this selectivity was enhanced by the attended orientation, and that these activities correlated with the monkeys' behavior. These results suggest that L-IPS neurons play important roles in the grouping and detection of objects comprised of discrete elements.

In the experiment described in Part 2, we examined which class of neurons is involved in the visual grouping. There are two major functional classes of cortical neurons, excitatory pyramidal neurons and inhibitory interneurons. However, it remains largely unknown how these two classes contribute to visual perception and cognition. Recently, several attempts have been made to classify extracellularly recorded neurons according to known differences in the waveforms of their action potentials (e.g., Mitchell et al., 2007, Neuron). These studies suggest that classification of neuron type will

provide valuable new information that could be crucial to understanding neural processing within local circuits in the cerebral cortex. We classified recorded neurons using the same procedure previously used by Mitchell et al. (2007), and examined how the resultant two classes of neurons contribute to visual grouping. We found that putative pyramidal neurons, which had broader action potentials, exhibited the selective responses to the target stimulus, and the selectivity was enhanced by attention. By contrast, putative inhibitory neurons, which had narrower action potentials, did not exhibit such selectivity or enhancement. These results suggest that different classes of parietal neurons contribute differently to the visual grouping of discrete elements.

In the experiment described in Part 3, we examined whether there is an anatomical basis for integration of visual signals. Classification of L-IPS neurons showed that pyramidal neurons exhibited selectivity for the target stimulus, and clearly indicates that L-IPS neurons signal information about the grouped stimulus to other cortical areas. Neurons in L-IPS may provide feedback signals and affect the activity related to visual grouping in the early visual area. However, no study has explored in detail the feedback projection related to the visual grouping. In an attempt to study the contribution of feedback projection on visual grouping, we examined whether there is an anatomical basis for integration of visual signals from both sides of blind spot (BS) by cortico-geniculate feedback neurons in V1. The blind spot is the region in the visual field that corresponds to the optic disk in the retina. No visual information exists in the blind spot because there are no photoreceptors within the optic disk. Nonetheless, we perceive color and/or patterns there that are the same as in the surrounding visual field. This phenomenon is known as perceptual filling-in, and closely related to the visual grouping. Neural mechanisms under perceptual filling-in at the blind spot has been

examined in detail (Komatsu 2006), and this provides a good physiological model to investigate the anatomical basis for integration of visual signals related to visual grouping. We injected biotinylated dextran amine (BDA) into a location adjacent to the blind spot region in V1. We observed that numerous BDA labeled axons traverse the neuron-free gap that retinotopically corresponds to BS within LGN. This indicates that visual signals from one side of BS are conveyed to the opposite side via a feedback connection. Cortico-geniculate feedback projection may integrate visual signals from around BS and contribute to perceptual filling-in at BS. This result provides anatomical evidence that feedback projection possesses architecture suited for binding information of discrete elements.

Part 1
Relationship between neural responses and visual grouping in the monkey parietal cortex

Introduction

Neurological studies of human patients suggest that the posterior parietal cortex plays a key role in visual grouping. For instance, patients with Balint's syndrome, who have bilateral damage to the parietal cortex, cannot perceive a visual scene as a whole; instead, they see only one of the multiple objects in a visual scene at a time. It has therefore been suggested that the posterior parietal cortex is involved in the integration of multiple objects and features and in global gestalt perception. (Warrington and James, 1967; Coslett and Saffran, 1991; Friedman-Hill et al., 1995; Himmelbach et al., 2009). It has also been reported that patients with unilateral damage to the parietal cortex have an impaired ability to allocate attention to promote visual grouping (Robertson et al., 1988), which suggests that the parietal cortex is also involved in visual grouping controlled by top-down attention. Many studies have shown that neurons in the lateral bank of the intra-parietal sulcus (L-IPS) are involved in spatial attention or selection and control of visually guided eye/hand movements (Gnadt and Andersen, 1988; Taira et al., 1990; Barash et al., 1991; Colby et al., 1996; Snyder et al., 2000; Shadlen and Newsome, 2001; Bisley and Goldberg, 2003, 2006). However, there have been no studies examining the involvement of parietal neurons in visual grouping.

To investigate the neuronal mechanisms underlying visual grouping, we designed a grouping detection task controlled by top-down attention, and then recorded neuronal activity from the L-IPS while the task was being performed by monkeys. The visual

stimuli consisted of multiple discrete dots, and the monkeys were required to detect the target defined by specific arrangements of the dots. Visual grouping was necessary for detection of the target, and we surmised that if L-IPS neurons are involved in visual grouping, they may selectively respond to the grouped objects. In addition, we manipulated the monkeys' attention to the grouping of the elements, and examined the effect of attention on the neuronal responses.

Materials and Methods

Visual stimuli and behavioral task

Two monkeys (*Macaca fuscata*, male, weighing 6.9-8.8kg) were used for these experiments. During the experiments, the monkeys sat in a primate chair and faced the screen of a CRT monitor. To examine the neural mechanisms underlying visual grouping affected by top-down attention, we designed a grouping detection task. The visual stimuli are shown in Fig.1A. They were composed of 5 square black or white dots (1.2 deg at the edge) arranged in a cross on a gray background. The spatial interval between the centers of neighboring dots was 2.4 deg, and the black and white dots (1.33cd/m^2 and 75cd/m^2 respectively, x= 0.313, y=0.329) had the same luminance contrast against the gray background (10cd/m^2, x= 0.313, y=0.329). Each visual stimulus contained either three white dots and two black dots or three black dots and two white dots. A total of 20 types of visual stimuli composed of different arrangements of dots were prepared and used in the behavioral task. In four of the 20 stimuli, three dots with the same contrast (either black or white) were aligned either horizontally or vertically and served as the target (Fig.1A top).

The target stimuli were characterized by two visual features: the orientation of the three dots with the same contrast that was either horizontal or vertical (columns in Fig.1A top) and the contrast of three-aligned dots, which was either white or black (rows in Fig.1A top). In the following text, we will refer to each target according to the combination of these two features (e.g., white-horizontal for the left-top target in Fig.1A). The remaining 16 stimuli, four of which are shown in Fig.1A bottom, were non-targets. The other 12 non-targets had the same pattern but different orientations separated by

90° each. The center position of the visual stimuli was 7.1° in eccentricity, and the polar angle was 22.5, 45.0, 157.5, 202.5, 225.0, 315.0 or 337.5° for monkey GG, or 337.5° for monkey FZ. In the early part of the experiment in GG, we also used three additional polar angles in a small number of neurons (328.3° in 7 neurons, 350.3° in 1 neuron, 9.7° in 1 neuron).

Figure 1B shows the time course of the behavioral task. In a trial, visual stimuli were presented multiple times interleaved with inter-stimulus intervals (ISIs). The monkeys made behavioral response via a lever. A trial started when a monkey pressed the lever, and a white fixation spot appeared at the center of the display. During the trial, the monkey was required to fixate on the spot and to maintain its eye position within a square fixation window. The size of the fixation window was 1.3-2.0 (mainly 1.3) deg at the edge for monkey GG and 1.6-2.0 (mainly 1.6) deg for monkey FZ. After 800 ms from the beginning of fixation, a visual stimulus was presented for 300 ms and then disappeared. This was followed by an ISI and then presentation of another visual stimulus. The ISI was 300 ms for monkey GG and 340 ms for monkey FZ. Visual stimuli were presented up to 4 times in one trial for monkey GG and 3 times for monkey FZ. A target was presented within a trial in 80% of the trials for monkey GG and 75% of the trials for monkey FZ. In the remaining 20% (or 25%) of the trials, a target was not presented. The target appeared only once or did not appear at all within a trial. The probability that the target would appear in each step of the stimulus presentation was the same (0.2/step for monkey GG, 0.25/step for monkey FZ). The monkeys had to release the lever within 600 ms after the onset of the target to obtain a liquid reward. In a trial in which no target was presented, the monkeys had to keep pressing the lever until the fixation spot disappeared to obtain a reward. If a monkey broke fixation or if it

released the lever even though a target did not appear, the fixation spot was turned off and an ITI began.

To detect the appearance of a target during a rapid sequence of stimuli, the monkeys were required to quickly discriminate the arrangement of dots. It is known that multiple elements of common contrast or multiple elements positioned in a row tend to be perceived as one object. Accordingly, the elements of a target are readily grouped in a bottom-up manner. On the other hand, it is also known that top-down attention affects visual grouping. In our task, if the monkeys knew the orientation (horizontal / vertical) or the contrast (white / black) of the forthcoming target in advance, we would expect that top-down attention would facilitate visual grouping of the dots. Therefore, in order to promote visual grouping by top-down attention in the present experiment, we included a predictable bias in the target orientation. Figure 1C shows a matrix indicating the relationship between the target orientation and the attended orientation. When the attended orientation is the same as the target orientation (valid condition), we would expect top-down attention to facilitate visual grouping. When the attended orientation differs from the target orientation (invalid condition), no such facilitation would be expected. It should be noted that monkeys can obtain a reward by detecting any target under either condition, regardless of whether the target has an attended or unattended orientation.

For monkey GG, attention was controlled by a visual cue: two short horizontal or vertical bars positioned symmetrically on opposite sides the fixation point. Horizontal cues were presented to the left and right of the fixation point, and vertical cues below and above the fixation point. Each bar was situated 1.0 deg at the near end from the fixation spot and had a length of 0.5 deg and a width of 0.1deg. The orientation of the

visual cue instructed the orientation to which attention should be directed. The proportion of trials in the valid condition was 80% for recordings from the left hemisphere and 90% for the right hemisphere. The remaining 20% or 10% of trials were in the invalid condition. The visual cue appeared 100 ms after the beginning of fixation and was presented throughout a trial. The orientation of the visual cue changed randomly from trial to trial. The presence of bars on opposite sides of the fixation point prevented the eye position from shifting toward a bar: deviation of the eye position during the trials were very small compared with the separation (1.0 deg) between the fixation spot and the end of the bar (mean $\pm$ SD: 0.02 $\pm$ 0.14 deg for the horizontal cue and 0.05 $\pm$ 0.12 deg for the vertical cue).

For monkey FZ, attention was controlled using a block design. Within a block of about 100 trials, a target with a particular orientation (horizontal or vertical) was presented in 90% of the trials (valid condition), and a target with the orthogonal orientation was presented in the remaining 10% (invalid condition). The attended orientation alternated between horizontal and vertical in serial blocks. In order to signal the new orientation at the beginning of a new block, only trials in the valid condition were run for about 20 trials. Because the monkey's attention was not stable during this period, the data obtained in these trials was excluded from the analysis.

Monkeys were also trained on a passive fixation task in which they only needed to maintain gaze on the fixation spot to get a reward.

Surgical procedures and recording

An eye coil and a head holder were implanted under sodium pentobarbital anesthesia using standard sterile surgical procedures. After training on the behavioral

task, a recording chamber was implanted on the skull. The recording chamber was placed at a position where we could horizontally insert electrodes into the L-IPS, the position of which was determined by magnetic resonance imaging (MRI) prior to the surgery. We targeted the L-IPS between the A3 and P3 stereotaxic coordinates. After surgery, antibiotics (Cefazolin, 0.06 g) were intramuscularly administered twice daily for 7 days to prevent infection. Monkeys were allowed to recover for more than 7 days after surgery; experiments were begun only after the monkeys have completely recovered. All procedures for animal care and experimentation were in accordance with the NIH Guide for the Care & Use of Laboratory Animals (1996) and were approved by our institutional animal experimentation committee.

Custom-written software running on three PC computers were used to control the presentation of the stimuli and the task schedule, and to record neural signals and eye positions. Visual stimuli were presented on a CRT monitor (frame rate at 100 Hz, Totoku Electric Co., LTD., Tokyo) situated at a distance of 57 cm from the monkey. Eye position was monitored using the scleral search coil technique (Robinson, 1963; Judge et al., 1980). We used tungsten microelectrodes (200 μm in diameter, 1-2.5 MΩ at 1 kHz, Frederick Haer & Co., Bowdoinham ME) that were inserted into the cortex using a hydraulic microdrive (MO-951, Narishige, Tokyo). Neural signals were amplified using a head amplifier and main amplifier (Nihon Kohden, Tokyo) and then sent to a PC. Neural signals and eye position were recorded on the PC's hard disk at sampling rates of 25 kHz and 1 kHz, respectively, for off-line analysis. The occurrence of spikes was monitored on-line and peristimulus time histograms (PSTHs) were generated during the recordings, which enabled us to evaluate the response properties of the recorded neuron. After recording, we confirmed the spike activity to be a single neuron using a

template-matching method, and then conducted off-line analysis using MATLAB (The MathWorks, Inc.).

We recorded 107 single neurons from L-IPS (GG 82, FZ 25). We roughly examined the receptive field in 72 of these neurons (GG 59, FZ 13) by presenting a square spot (1-2 deg in size) at various positions in the visual field during a passive fixation task. Monkey GG was trained the grouping detection task at seven different positions in the visual field, and we aimed to determine the position to present the stimuli in the grouping detection task based on this receptive field mapping. For the remaining neurons, we did not test the receptive field and determined the target position based on the records from the nearby sites. For monkey FZ that was trained to perform the grouping detection task only at one position, we confirmed that the receptive field overlapped with the target position (n=13). For the remaining neurons, we confirmed that the visual response is evoked at the target position by presenting a visual stimulus (n=9). We found that neurons recorded in more posterior part tended to have receptive fields in the upper visual field, which is consistent with an earlier report (Ben Hamed et al. 2001). However, in either monkey, we did not attempt to scrutinize the boundary of the receptive field.

Data analysis

The minimum number of repetitions of each stimulus accepted for analysis was five. Typically, more than seven repetitions of each stimulus condition were carried out for each neuron. Firing rates were computed within the period between 50 and 250 ms after stimulus onset. This timing corresponded roughly to the minimum latency of the light sensitive LIP neurons (Barash et al., 1991; Bisley et al., 2004) and the minimum

reaction time, respectively. Monkeys released the lever earlier than the latter timing in only a very small number of trials (0.29% for monkey GG, 0.35% for monkey FZ). Only neurons that showed a significant increase in activity to at least one target stimulus ($p < 0.05$, *t* test) were used for analysis. Although a comparison between correct and error trials would be of interest, the number of error trials for each stimulus was too small to allow systematic analysis. Therefore, we analyzed only data obtained in correct trials.

The response selectivity of each neuron was evaluated statistically using three-factor analysis of variance (ANOVA) with target orientation (horizontal or vertical), target contrast (white or black) and attended orientation (horizontal or vertical) as the main factors. Before the ANOVA, we applied a square-root transformation to transform the distribution of firing rates into a normal distribution.

We performed a rank analysis to determine how the responses to targets differ from those to non-targets. There were 40 stimulus conditions (i.e., 20 types of stimulus presented in 2 attended orientations). These stimulus conditions were ranked according to the order of the response magnitudes. The stimulus condition ranked 1st was the stimulus condition in which the strongest response was evoked among the 40 stimulus conditions.

There were 4 targets made of a combination of two target orientations (horizontal or vertical) and two target contrasts (white or black). To determine whether these features were expressed in the neural activity, we quantified the magnitude of selectivity using the following equations. First, we computed the difference in responses between different target orientations (DBO) and the difference in responses between different target contrasts (DBC) as follows:

$$DBO = | (WHt + BHt) - (WVt + BVt) | / 2,$$

DBC = | (*WHt* + *WVt*) - (*BHt* + *BVt*) | / 2

where *WHt, BHt, WVt* and *BVt* respectively represent the response to the target in which white dots are aligned horizontally, black dots are aligned horizontally, white dots are aligned vertically, and black dots are aligned vertically. DBO and DBC were calculated in each attention condition separately.

Next, we quantified the selectivity of each neuron for the target orientation and the target contrast by normalizing the response difference between relevant features to the sum of the responses to all features as follows:

Orientation selectivity index = | (*WHt* + *BHt*) - (*WVt* + *BVt*) | / (*WHt* + *BHt* + *WVt* + *BVt*)

Contrast selectivity index = | (*WHt* + *WVt*) - (*BHt* + *BVt*) | / (*WHt* + *BHt* + *WVt* + *BVt*)

Each selectivity index takes a value between 0 and 1, and a larger value corresponds to stronger selectivity.

Finally, in order to determine whether the magnitude of selectivity was modulated by attention, we calculated a modulation index as follows:

$$\text{Attention modulation index} = (DBO_{valid} - DBO_{invalid}) / (DBO_{valid} + DBO_{invalid}) \quad (1)$$

where DBO_{valid} and $DBO_{invalid}$ indicate the value of DBO in the valid condition and that in the invalid condition, respectively. Modulation indexes ranged between -1 and 1, with a positive value indicating that the selectivity is stronger in the valid condition than in the invalid condition.

Histology

In one monkey (GG), we confirmed the positions of the recordings histologically. After all the experiments were completed, the monkey was deeply anesthetized with pentobarbital sodium and then transcardially perfused with a 4% paraformaldehyde

solution. Serial 50-μm sections were cut in the coronal plane using cryostat (CM3050, Leica, Germany), and every other section was stained with Cresyl violet. The brain slices were then examined microscopically, and histologically identified electrode tracks were superimposed on the nearest representative slice at a 1-mm interval. A dense array of electrode tracks were found in the middle portion of the L-IPS (left hemisphere: A0-P4, right hemisphere: A1-P2, Fig. 2). The other monkey (FZ) is still alive. In this monkey, X-ray images and MRI were used to confirm that the recordings were made from the L-IPS between the A3 and P3 stereotaxic coordinates.

Results

Monkey behavior during a grouping detection task

We recorded 107 single neurons from the L-IPS of two monkeys (82 neurons from monkey GG, 25 neurons from monkey FZ). Figure 3 summarizes the behavioral performance of the monkeys during the period the neural activities were being recorded. Figure 3A shows the distribution of reaction times in the valid (red) and invalid (blue) conditions. Reaction time was defined as the interval between the onset of the target and the lever release. For both monkeys, the reaction time was, on average, significantly shorter in the valid condition than in the invalid condition (monkey GG: median = 328.6 ms vs. 349.3 ms, valid vs. invalid, n= 24265 trials, $p < 0.001$, Mann-Whitney test, monkey FZ: 315.3 ms vs. 342.5 ms, n= 8252 trials, $p < 0.001$). Similarly, the average detection rates across the recording sessions for each neuron were significantly higher in the valid condition than in the invalid condition (monkey GG: 96.9% vs. 86.8%, valid vs. invalid, n= 76 sessions, $p < 0.001$, paired *t* test; monkey FZ: 98.9% vs. 91.6%, n= 24 sessions, $p < 0.001$) (Fig. 3B). The number of sessions differs from the number of neurons because two individual neurons were recorded simultaneously in seven sessions (monkey GG: 6, monkey FZ: 1). Comparison of the reaction times and detection rates showed that behavioral performance was better in the valid condition than in the invalid condition, which confirms that in both monkeys attention was guided to the target orientation instructed by the experimenter.

Comparison of the responses of L-IPS neurons to target and non-target stimuli

We found neurons in the L-IPS that selectively responded to the visual stimuli during the grouping detection task. Figures 3A and B show the responses of a representative neuron as spike density functions. This neuron responded strongly to some of the stimuli but not to others. Given that activity in the posterior parietal cortex is known to be closely related to spatial attention and behavioral selection, one possibility is that the selective responses discriminate between the target and non-target stimuli. However, the recorded L-IPS neurons did not show selective responses distinguishing target from non-target stimuli. The neuron whose behavior is summarized in Fig. 4A and B responded strongly to some targets but not to others. In addition, this neuron showed strong responses to some of the non-targets as well, indicating that it did not discriminate between the target and the non-target.

To illustrate this more clearly, the response profile for this neuron is shown in Fig. 4C. The responses to all target stimuli in both the valid and invalid conditions, as well as the responses to all non-target stimuli, are plotted. The mean of the response magnitudes for the four targets in the valid condition did not significantly differ from that for non-targets (mean $\pm$ SD: 32.0 $\pm$ 20.9 spk/s for targets, 32.2 $\pm$ 9.53 spk/s for the non-targets, $p = 0.97$, *t* test), which indicates that, on the whole, this neuron did not discriminate target from non-target. Instead, we found that there was an interesting difference between the distributions of the responses to targets and non-targets. The responses to targets in the valid condition were located at the two extremes of the response distribution. In other words, this neuron not only responded most strongly to some targets, it also responded most weakly to other targets. In the invalid condition, the responses to targets were distributed in a smaller range (mean $\pm$ SD: 31.8 $\pm$ 10.1 spk/s) than in the valid condition.

Figure 4D shows the results of a rank analysis in which all the stimulus conditions were sorted according to the magnitude of the response: rank #1 was the strongest response, while rank #40 was the weakest. The responses to the target stimuli in the valid condition (red bars) were ranked at #1, #4, #35 and #40, and were thus positioned at the two extremes. This tendency was generally observed across the recorded neurons. Figure 5 shows the distribution of ranks for all four target stimuli in the valid (red) and invalid (blue) condition for all 107 neurons recorded. The distribution was clearly skewed toward both the smallest (strongest response) and largest (weakest response) ranks, and significantly deviated from the uniform distribution (gray line). This bias toward the two extremes was apparent both in the valid condition and in the invalid condition.

The results summarized above suggest the possibility that L-IPS neurons are selective for some of the visual features included in the target stimuli, namely the target contrast or the target orientation (Fig.1A). In addition, the difference between the valid and invalid conditions observed in Fig. 4 suggests that attention to target orientation may affect the neural responses. The results of an ANOVA were consistent with this impression. Ninety-three of the 107 recorded neurons (68 of 82 neurons in monkey GG, 25 of 25 neurons in monkey FZ) showed a significant main effect ($p < 0.05$) of selectivity for either the target orientation or target contrast. Of those 93 neurons, 81 (87.1%; 58 of 68 neurons in monkey GG and 23 of 25 neurons in monkey FZ) showed a significant main effect of target orientation, 62 (66.7%; 46 of 68 neurons in monkey GG and 16 of 25 neurons in monkey FZ) showed a significant effect of target contrast, and 50 (53.8%; 36 of 68 neurons in monkey GG and 14 of 25 neurons in monkey FZ) showed a significant main effect of both target orientation and target contrast. In 31 neurons

(33.3%; 23 of 68 neurons in monkey GG and 8 of 25 neurons in monkey FZ), the attended orientation was a significant main factor. To fully understand how L-IPS neurons responded to target stimuli and how attention affected the responses, we next examined in more detail the selectivity of the recorded L-IPS neurons for the target features and the effect of attention. In the following parts of this paper, we will focus on the population of 93 neurons showing statistically significant selectivity for target orientation or contrast in the aforementioned ANOVA.

Responses to the target stimuli: example neurons

Figure 6 shows the responses of two representive neurons to the target stimuli. In both neurons, target orientation was a significant main factor in the ANOVA. The neuron shown in Fig. 6A-C was recorded in monkey GG (the responses of the same neuron are depicted in Fig. 4). As can be seen in Fig. 6A, in both the valid (red) and invalid (blue) conditions, this neuron responded strongly to targets in which dots with the same contrast were aligned horizontally (horizontal targets), whereas it responded only weakly to targets in which dots with the same contrast were aligned vertically (vertical targets). This preference did not depend on the contrast, as similar responses were observed whether the aligned dots were black or white. Figure 6B shows the response magnitudes computed during the period from 50 to 250 ms after stimulus onset in each condition. To quantitatively evaluate this neuron's selectivity, we computed the difference in the responses to targets with different orientations (DBO, see method), as well as the difference in the responses to targets with different contrasts (DBC). The left panel in Fig. 6C shows the computed DBOs depicted as vertical bars corresponding to the differences between the mean responses to the horizontal targets and those to the

vertical targets. The red and blue bars depict the DBOs obtained in the valid and invalid conditions, respectively. The right panel in Fig. 6C shows the computed DBCs corresponding to the differences between the mean responses to the white and black targets. The values of DBO and DBC were, respectively, 35.5 and 1.9 spk/s in the valid condition and 13.8 and 9.3 spk/s in the invalid condition. DBO was greater than DBC in both attention conditions, confirming the notion that this neuron was more selective for target orientation than target contrast.

We next assessed the influence of top-down attention on the magnitude of the selectivity for target orientation and for target contrast. The responses to the horizontal targets were stronger in the valid condition than in the invalid condition and, conversely, the responses to the vertical target were stronger in the invalid condition than in the valid condition. As a result, DBO was greater in the valid condition than in the invalid condition (vertical bars on the left panel of Fig. 6C). This suggests that the selectivity for the target orientation was enhanced when the target orientation was the same as the attended orientation.

The neuron shown in Fig. 6D-F was recorded from monkey FZ. This neuron responded more strongly to the vertical target than to the horizontal target in both attention conditions, and selective responses were not dependent on the target contrast (Fig. 6D and E). The values of DBO and DBC were, respectively, 14.3 and 2.2 spk/s in the valid condition and 6.1 and 0.6 spk/s in the invalid condition (Fig. 6F). Thus DBO was greater than DBC in both attention conditions, which indicates this neuron was also more selective for target orientation than target contrast. In addition, DBO was greater in the valid condition than in the invalid condition, indicating that attention enhanced the orientation selectivity.

Thus the responses to the targets of the two example neurons depicted in Fig. 6 had two characteristics in common, even though they preferred different orientations: 1) the selectivity for target orientation was greater than that for target contrast; and 2) the selectivity was enhanced when the target orientation matched the attended orientation (valid condition). These two characteristics were commonly observed across the recorded L-IPS neurons. In the following sections, we will first describe the feature selectivity and then describe the effect of attention on the population activity of L-IPS neurons.

Selective responses to target features: population analysis

To quantify the degree of selectivity for each visual feature, we calculated an orientation selectivity index and a contrast selectivity index for each neuron. Comparisons of the two selectivity indexes across the population of L-IPS neurons are shown in Fig. 7. The results obtained from the two monkeys are shown separately in the left and right columns. In the valid condition (panel A), a majority of the data points (71.0%; 46 of 68 neurons in monkey GG, 20 of 25 neurons in monkey FZ) were located above the diagonal line, indicating that the orientation selectivity tended to be stronger than the contrast selectivity. In both monkeys, the mean orientation selectivity index (0.28 for monkey GG, 0.37 for monkey FZ) was significantly larger than the mean contrast selectivity index (0.14 for monkey GG, 0.14 for monkey FZ; $p < 0.001$ for both monkeys, Wilcoxon signed-rank test).

The results obtained in the invalid condition (Fig. 7B) are essentially the same as in the valid condition. In more than half of the neurons (63.4%; 44 of 68 neurons in monkey GG, 15 of 25 neurons in monkey FZ), the data points were located above the diagonal

line, and again the mean orientation selectivity index (0.23 for monkey GG, 0.29 for monkey FZ) was larger than the mean contrast selectivity index (0.16 for monkey GG, 0.16 for monkey FZ; p = 0.054 for monkey GG, p = 0.010 for monkey FZ, Wilcoxon signed-rank test). It should be noted that if a neuron responded to only one target stimulus, the orientation selectivity index would equal the contrast selectivity index, and the data point would fall on the diagonal line in the scatter plot. Therefore, these results confirm that this population of L-IPS neurons exhibit greater selectivity for a target's orientation than for its contrast in both attention conditions, and indicate that the biased distribution of target stimulus ranks shown in Fig. 5 reflects this selectivity for target orientation.

Effect of attention: population analysis

The example neurons depicted in Fig. 6 showed greater orientation selectivity in the valid condition than in the invalid condition. To determine whether this is characteristic across the population of L-IPS neurons, we computed an attention modulation index for each neuron, the distribution of which is shown in Fig. 8. For both monkeys, the mean attention modulation index (0.10 for monkey GG, 0.15 for monkey FZ) was significantly larger than zero (p = 0.044 for monkey GG, p = 0.014 for monkey FZ, *t* test), indicating that the selectivity for target orientation was greater in the valid condition than in the invalid condition. And if we consider only the cells that showed a significant main effect of target orientation in the ANOVA, the mean attention modulation index (0.18 for monkey GG, 0.19 for monkey FZ) was even larger (Fig.8, dark gray bars). These results are consistent with the idea that selectivity for target orientation is enhanced in the valid condition. To examine whether attention to the target orientation modulates the

selectivity for target contrast, we computed an attention modulation index for contrast by replacing DBO in equation (1) with DBC. Unlike the index for target orientation, the attention modulation index for contrast selectivity was not significantly different from zero (-0.03, p = 0.72 *t* test in monkey GG; -0.05, p = 0.74 in monkey FZ). This means that whereas attention toward target orientation increases the selectivity for target orientation, it has no effect on selectivity for target contrast.

Attention to orientation was guided by a different paradigm with each monkey. A visual cue was used with monkey GG, which made it difficult to completely separate the effect of attention from the influence of the sensory input on neuronal activity. In the other monkey (FZ), however, attention was guided by a block design, and no visual cue was presented, which enabled us to rule out the possibility that the visual cue affected the observed neuronal activity. That we observed similar neural selectivity and attentional modulation in both monkeys means that it is very likely that differences in the response modulation between the valid and invalid conditions are due to the effect of attention, not the influence of visual sensory input.

Mechanism of the attentional modulation

The analysis described so far showed that the selectivity for target orientation was enhanced in the valid condition. To better understand the mechanism underlying that enhancement, we next analyzed the responses to the target stimuli to determine how they are affected by the attended orientation. Figure 9A shows the responses of the same neuron depicted in Fig. 6A-C, but in this case the responses were sorted according to the attended orientation. The responses to the target stimuli were consistently stronger when the monkey directed its attention to the horizontal orientation

(open circles) than when attention was directed to the vertical orientation (filled circles). Similar response modulation that was dependent on the attended orientation was also observed in responses to the non-target stimuli (Fig. 9B). The average neuronal response elicited when the monkey directed its attention to the preferred orientation (open triangle, 38.8 ± 7.48 spk/s) was significantly greater than that elicited when attention was directed to the non-preferred orientation (filled triangle, 25.6 ± 6.23 spk/s), ($p < 0.01$, *t* test). This suggests that attention toward a particular orientation biased the magnitude of this neuron's response. Considering that this example neuron preferred the horizontal target (Fig. 6A), we think that the response to the target was increased when the monkey directed its attention to the preferred orientation and reduced when attention was directed to the non-preferred orientation. Such response modulation can naturally explain the enhancement of neural selectivity in the valid condition. Because the attended orientation and the stimulus orientation are the same in the valid condition, the responses to target stimuli with the preferred orientation will increase, whereas those to target stimuli with the non-preferred orientation will decrease, which will enhance the selectivity for the target orientation.

Response enhancement was generally observed in the recorded L-IPS neurons when attention was directed toward the preferred orientation. In Fig. 10A, the results obtained from the two monkeys are shown separately in the left and right columns. The preferred orientation was defined as the orientation in which the average firing rate was higher in the valid condition, and the non-preferred orientation was the orthogonal orientation. The average responses to the target when the monkeys directed their attention to the preferred orientation (open triangle, 24.3 spk/s in monkey GG, 22.1 spk/s in monkey FZ) were significantly higher than those when attention was directed to

the non-preferred orientation (filled triangle, 22.8 spk/s in monkey GG, 19.8 spk/s in monkey FZ; $p < 0.001$ in both monkeys, paired *t* test). In addition, the result obtained for the response to the non-target was similar to the response to the target (Fig. 10B). The average responses to the non-target obtained when the monkeys directed their attention to the preferred orientation (open triangle, 23.0 spk/s in monkey GG, 21.3 spk/s in monkey FZ) were significantly higher than those obtained when attention was directed to the non-preferred orientation (filled triangle, 21.0 spk/s in monkey GG, 18.0 spk/s in monkey FZ; $p < 0.001$ in both monkeys, paired *t* test). Thus the population of L-IPS neurons responded more strongly when the monkeys directed their attention to the preferred orientation than when their attention was directed to the non-preferred orientation.

The responses of the neuron depicted in Fig. 9 were enhanced when the monkey directed its attention to the preferred orientation, regardless of whether the target stimulus was preferred or non-preferred. To determine whether this pattern of response modulation is characteristic of L-IPS neurons, we compared responses to the same target in the preferred orientation (preferred target) or the non-preferred orientation (non-preferred target) while attention was being directed toward the preferred orientation for each neuron or toward the orthogonal orientation. Figure 11A shows the comparison of these responses for each neuron recorded from the two monkeys. Each circle represents the response to the preferred (horizontal axis) and non-preferred (vertical axis) targets, with the open and solid circles representing attention to the preferred and non-preferred orientations, respectively. The two data points (open and solid circles) obtained from the same neuron are connected by a line segment. In this diagram, if the response of a given neuron was stronger when attention was directed

toward the preferred orientation than when it was directed toward the orthogonal orientation, the distance from the origin of the coordinates will be larger for the open circle than the solid circle. In addition, if the responses to the preferred and non-preferred targets are similarly modulated by the change in the attention condition, the line connecting the open and solid circles will be parallel to the diagonal line. Although the effects of the attention condition varied from neuron to neuron, there was a general tendency for the response modulation to be similar between the preferred and non-preferred targets. For each neuron, response modulation that was dependent on the attention condition can be represented as a vector corresponding to the positional difference between the open and solid circles: the horizontal component of the vector represents the magnitude of the response modulation of the preferred target, while the vertical component represents that for the non-preferred target. Figure 11B shows vector representations of the response modulation of all the recorded L-IPS neurons. In both monkeys, the average of the modulation (thick-black line) pointed to the first quadrant – i.e., the average magnitude of the response modulation for the preferred target was significantly larger than zero (1.85, $p = 0.01$ *t* test in monkey GG; 2.24, $p = 0.02$ in monkey FZ); likewise, that to the non-preferred target was also significantly larger than zero (1.26, $p = 0.02$ *t* test in monkey GG; 2.29, $p < 0.01$ in monkey FZ). This means that attention directed toward the preferred orientation for a given neuron tended to increase responses to both the preferred and non-preferred targets. A large majority of neurons pointing to the first quadrant in Fig.11B (32 of 37 in monkey GG, 14 of 15 in monkey FZ) exhibited enhanced selectivity for the target orientation in the valid condition, during which the attention modulation index was larger than zero (Fig. 8), whereas few neurons pointing to other quadrants (6 of 31 in monkey GG, 2 of 10 in

monkey FZ) exhibited such enhancement of selectivity. This suggests that the enhancement of the selectivity for the target orientation in the valid condition was mainly due to the greater magnitude of the responses to the target stimuli obtained when the monkeys directed their attention to the preferred orientation.

Time course of the orientation selectivity and attentional modulation

Figure 12A illustrates the time course of the population activity for all the neurons (n=93) in the different stimulus conditions. Red and blue lines represent the valid and invalid conditions, respectively, while the solid and broken lines represent the preferred and non-preferred orientations. The order of the response amplitudes is consistent with the results described above. When the time courses of the responses were compared, the difference in the responses between the preferred (solid line) and non-preferred (broken line) orientations occurred earlier in the valid condition (red) than in the invalid condition (blue). This can be seen more clearly in Fig. 12B, which shows the differences between the responses to the preferred and non-preferred orientations. In the valid condition (red), the response differences arose 50 ms after stimulus onset and reached a maximum at 170 ms. In the invalid condition (blue), by contrast, the differences arose 100 ms after stimulus onset and reached a maximum at about 200 ms. We computed the time at which the response difference reached its half-maximum after stimulus onset. In 19 neurons this time was less than 30 ms in one or the other attention condition, as the maximum was positioned around the stimulus onset. These neurons were excluded from the following analysis because the latencies were unreliable. For the remaining neurons, the average time at which the response difference reached half maximum in the valid condition (mean ± SD: 115.6 ± 37.8 ms) was about 40 ms shorter than that in

the invalid condition (152.1 ± 44.8 ms, p <0.0001 paired *t* test, n=74), which means that orientation selectivity arose earlier in the valid condition than in the invalid condition.

In summary, we found that the orientation selectivity of neurons was enhanced and arose earlier in the valid condition and, correspondingly, the monkeys exhibited better behavioral performance. Apparently, selective responses to the target orientation of L-IPS neurons correlate with the behavioral performance in the monkey.

Correlation between neural selectivity and behavioral performance

To determine whether there was a trial-by-trial relationship between L-IPS neuron activity and the behavioral performance, we computed the correlation between the neuronal firing rates and the monkeys' reaction times for each target stimulus condition in each trial. The number of spikes occurring within the period from 80 to 180 ms after stimulus onset, during which there was a large difference in neural selectivity for the target orientation between the valid and invalid conditions (e.g. Fig.12B), were converted to firing rates. Figure 13A shows the correlation between the trial-by-trial firing rate and the reaction time for the neuron depicted in Fig. 6A-C. The preferred orientation of this neuron was horizontal. When the target stimulus had the preferred orientation (horizontal), the reaction time was negatively correlated with the firing rate (a and c), although the correlation was not significant for the black horizontal target (c). By contrast, when the target stimulus had the non-preferred orientation (vertical), the reaction time was positively correlated with the firing rate (b and d). This indicates that the increase in the response to the preferred stimulus shortened the reaction time, while the increase in the response to the non-preferred stimulus delayed the reaction time. This tendency was observed across the population of L-IPS neurons, and Fig. 13B

shows the distribution of the correlation coefficients computed for the responses to the preferred (Fig.13B a) and non-preferred (Fig. 13B b) orientations. The correlation coefficient was, on average, significantly less than zero for the preferred orientation (mean = -0.087, $p < 0.00001$, *t* test) and significantly larger than zero for the non-preferred orientation (0.071, $p < 0.00001$, *t* test). The same results were obtained when the correlation coefficient was computed for responses in only the valid condition (preferred orientation; mean = -0.072, $p < 0.00001$, non-preferred orientation; 0.052, $p = 0.00003$, *t* test). These results are consistent with the idea that the orientation-selective responses of L-IPS neurons closely correlate with the monkey's behavior.

Responses to conventional bar stimuli

The present study indicates that L-IPS neurons encode the orientation of the target stimuli in the grouping detection task that are composed of discrete dots. Do these neurons encode the orientation of the conventional bar stimuli as well? To examine this problem, we also tested the responses to conventional bar stimuli during the fixation task in 36 neurons (20 of 82 neurons in monkey GG, 16 of 25 in FZ). The spatial extent of the bar stimulus (1.2 x 6 deg) matched that of the three dots aligned horizontally or vertically in the target stimuli used in the grouping detection task. We tested the responses of each neuron by using four bars generated by combining 2 orientations (horizontal or vertical) and 2 contrasts (black or white). Most of these neurons (72.2 %, 26 of 36) showed significant increase in the response to at least one of the bar stimuli although the responses tended to be weaker than in the grouping detection task (mean $\pm$ SD, 31.7 $\pm$ 20.2 spks/s for the responses to the preferred conventional bar stimulus in the fixation task vs. 36.6 $\pm$ 21.4 spks/s for the preferred target stimulus in the grouping

detection task). In these 26 neurons that exhibited significant responses to the conventional bar stimuli, a half (13 of 26) showed significant selectivity to the bar orientation ($p < 0.05$, 2-factor ANOVA) and one-third (9 of 26) showed significant selectivity to the bar contrast. All but one neurons (12 of 13) that showed orientation selectivity to the conventional bar stimuli also exhibited significant orientation selectivity to the target stimuli during the grouping detection task. The preferred orientation was consistent between the two conditions in most cases (10 of 12). These results indicate that some of the L-IPS neurons recorded in the present study can also encode the orientation of the conventional bar stimulus as well as the orientation of the stimulus composed of discrete elements.

Discussion

We recorded the activities of single neurons in the L-IPS while two monkeys performed a grouping detection task. We found that L-IPS neurons selectively responded to target orientation, that this selectivity was enhanced when the target orientation matched the attended orientation, and that the orientation-selective responses correlated with the monkeys' behavior. This suggests that L-IPS neurons play important roles in the grouping and detection of objects comprised of discrete elements.

Grouping of discrete elements in the L-IPS

Numerous studies have shown that the posterior parietal cortex participates in spatial attention and selection/intention of goal-directed movements (Barash et al., 1991; Colby et al., 1996; Snyder et al., 2000; Shadlen and Newsome, 2001; Bisley and Goldberg, 2003, 2006; Balan and Gottlieb, 2006). In our task, L-IPS neurons were expected to show stronger responses to target stimuli than to non-target stimuli because the monkeys' spatial attention should shift toward the target location when they detected the target. This is not what we observed, however. Instead, the responses to the target were biased toward the highest and lowest levels among the responses to all stimuli, and selectively represented the target orientation, which was a feature formed by the grouping of discrete dots. Each element of the stimulus is a black or white square; it gives no information about whether the entire stimulus is the target or the non-target. The size of each element is 1.2 deg at the edge, and the extent of the entire stimulus is 6 deg. At an eccentricity of 7.1 deg, where the stimulus was presented, the

average size of the receptive field is 1.5 deg in V1, 3.2 deg in V2, and 3.9 deg in V3 (Gattass et al, 1981; Gattass et al, 1988). Consequently, the receptive fields of individual neurons in V1 - V3 are too small to determine whether a stimulus is the target or the non-target. The receptive fields of V4 neurons are large enough to represent the entire stimulus, but it is not known whether the activity of V4 neurons is related to the grouping of aligned dots. By contrast, we found the activity of neurons to be selective for the target orientation in the L-IPS.

It is reported that L-IPS neurons can acquire the selectivity for the visual features (e.g., color and motion direction) that are important for performance of a behavioral task (Toth and Assad, 2002; Freedman and Assad, 2006). In the present study, each stimulus contained two visual features, orientation and contrast. Of these, only orientation was diagnostic for detection of the target. Presumably, the selectivity of L-IPS neurons for the orientation of the aligned dots developed as a result of the learning, and was involved in the performance of the grouping detection task.

Attentional control of visual grouping

Visual grouping is facilitated by prior knowledge via top-down attentional control. In the present study, we found that the detection of a grouped target by L-IPS neurons is controlled by prior knowledge of the target orientation. We found that L-IPS neurons tended to respond more strongly when a monkey directed its attention to the preferred orientation of the neuron under study. Such response modulation enhanced the selectivity for the target orientation in the valid condition. These results suggest that the neural population preferring the horizontal orientation and that preferring the vertical orientation are selectively enhanced or suppressed by the top-down signal in a

reciprocal manner. This pattern of attentional modulation agrees well with the biased-competition model of selective attention (Desimone and Duncan, 1995; Reynolds and Desimone, 2003). Notably, patients with damage to their parietal cortex show an impaired ability to employ prior knowledge for visual grouping (Robertson et al., 1988). The absence of the facilitated grouping of objects through attention to the relevant feature, like that observed in the present study, could underlie the deficits in these patients.

Perception of the global shape of hierarchically organized stimuli is known to require visual grouping (Navon, 1977), but the findings of imaging studies employing such stimuli with humans and monkeys have been inconsistent. Some studies have shown that directing attention to stimuli on either the global or local level activated the occipital prestriate cortex or the inferior temporal cortex (Heinze et al., 1998; Sasaki et al., 2001; Tanaka et al., 2001). In contrast, when attention was switched between the global and local levels, the parietal cortex was activated (Fink et al., 1996). It has been suggested that, in normal subjects, the global advantage automatically generates global gestalt perception, which will mask activity related to global perception if activities are simply contrasted between local and global attention conditions (Himmelbach et al., 2009). The present findings suggest that the parietal cortex plays an important role in the selection of global gestalt objects from among multiple candidates.

Relation to the functional organization of the IPS

The cortex in the L-IPS region is thought to be comprised of multiple areas having different functions (Lewis and Van Essen, 2000; Grefkes and Fink, 2005). Selectivity for object shape has been observed in both the AIP and LIP, which are adjacently situated

within the L-IPS (Sereno and Maunsell, 1998; Murata et al., 2000). LIP has been usually identified based on the activities during a memory-guided saccade task. Because we did not employ this task, we do not know whether the recordings made in the present study were from within the AIP or LIP. Judging from the reported stereotaxic coordinate of these areas (Toth and Assad, 2002; Sereno and Amadar, 2006; Borra et al., 2007; Janssen et al., 2008), our recording site (A3-P4) seems mainly situated in the anterior part of LIP and possibly includes a part of AIP. Important functional aspects of neurons within those two areas are activities related to saccadic eye movements or complex hand manipulation. However, neuronal responses in the present study have no relevance to either of these, as the monkeys maintained fixation and responded with a simple lever press/release. Thus our findings reveal an important new aspect of the response properties of neurons in the L-IPS involved in visual grouping.

Shape selectivity in the ventral and dorsal streams

It was previously reported that neurons exhibiting selectivity for an object's shape are present in areas positioned within both the ventral stream (Desimone et al., 1984; Tanaka et al., 1991; Pasupathy and Connor, 2002) and dorsal stream (Sereno and Maunsell, 1998; Murata et al., 2000; Durand et al., 2007; Janssen et al., 2008). Previous studies have shown that the way shape is encoded differs between the dorsal and ventral visual stream areas (Lehky and Sereno, 2007; Janssen et al., 2008). In one study, Janssen and colleagues (2008) showed that LIP neurons exhibit only minimal size and position invariance and concluded that shape selectivity in the LIP radically differs from that in the ventral visual areas. They suggested that LIP neurons do not provide an abstract representation of 2-dimensional shapes; instead, the shape

selectivity of these neurons may be related to accomplishing appropriate eye movements or grasping.

There may be an additional difference between the shape selectivities of neurons in the dorsal and ventral stream areas: our present results have shown that neurons in the L-IPS exhibit shape selectivity for objects formed by the visual grouping of isolated elements. On the other hand, recent studies have shown that the shape selectivity of neurons in areas within the ventral stream (e.g., V4 and the inferior temporal cortex) are based on the orientation and curvature of the object contour (Connor et al., 2007). This raises the interesting possibility that the encoding of shape in ventral stream areas is based on an analysis of the continuous contour, whereas in dorsal stream areas it is based more on the visual grouping of the discrete elements. Using normal human subjects, Xu and Chun (2007) recently showed that the grouping of discrete elements reduced activity in the inferior parietal cortex, while activity in the LOC, which is thought to belong to the ventral stream, was unchanged. This suggests that the inferior parietal cortex is involved in the encoding of visual grouping, but the LOC is not, which is consistent with the idea summarized above and emphasizes that the L-IPS is specifically involved in visual grouping. Interestingly, those authors suggested that the encoding of grouping within the L-IPS occurs automatically, without attention, as grouping was irrelevant to the main task performed by the subjects. Similarly, in our present experiment, selectivity for the target orientation was clearly observed in the invalid condition, during which the monkey's attention was directed to a different orientation. This suggests that the neural mechanism responsible for the development of the orientation selectivity of L-IPS neurons can be driven by bottom-up visual signals. Thus the L-IPS may be regarded as the site where top-down signals facilitating the

grouping of visual elements through attention or expectation meet the bottom-up visual signals consistent with the Gestalt principles of grouping.

L-IPS neurons encoding visual grouping may in turn facilitate neuronal activity related to visual grouping in the early visual areas. Neuronal activity in V1 is modulated by the presentation of visual stimuli in the receptive field surround, and it has been suggested that this contextual modulation is related to the visual grouping (Gilbert et al., 2000). In addition, this V1 activity can be modulated by attention. Presumably, L-IPS neurons provide feedback signals to the early visual areas and affect the contextual modulation there. A recurrent circuit between the L-IPS and early visual areas may be critical for visual grouping through the interchange of feedforward and feedback signals.

Part 2
Putative pyramidal neurons and interneurons in the monkey parietal cortex make different contributions to the performance of a visual grouping task

Introduction

Although it is known that there are many functional classes of cortical neurons, which include excitatory pyramidal neurons and inhibitory interneurons, it remains largely unknown how those two classes each contribute to visual perception and cognition. Recently, several attempts have been made to classify extracellularly recorded neurons according to known differences in the waveforms of their action potentials (e.g., Mitchell et al., 2007). These studies revealed interesting differences between putative pyramidal neurons and interneurons with respect to their relation to the numerical representation, task selectivity and the effects of attention and working memory (Diester and Nieder 2008; Johnston et al. 2009; Mitchell et al. 2007; Rao et al. 1999). They also suggest that classification of neuron type will provide valuable new information that could be crucial to understanding neural processing within local circuits in the cerebral cortex.

We found that L-IPS neurons exhibit selectivity for grouped stimuli, and that the strength of the selectivity is affected by attention, which suggests L-IPS neurons play an important role in visual grouping affected by top-down attention. It remains unknown, however, how different types of neurons are involved in visual grouping.

Here, we classified recorded neurons using the same procedure previously used by Mitchell et al. (2007), and examined how the resultant two classes of neurons contribute

to visual grouping. We found that putative pyramidal neurons, which had broader action potentials (Br), exhibited selectivity for the orientation of the target stimulus, and the selectivity was enhanced by attention. By contrast, putative inhibitory neurons, which had narrower action potentials (Nr), did not exhibit such selectivity or enhancement. Instead, these neurons responded more strongly to the target stimuli than to the non-targets. These results suggest that different classes of parietal neurons contribute differently to the visual grouping of discrete elements.

Materials and Methods

Two monkeys (*Macaca fuscata*, male, weighing 6.9-8.8 kg, monkey GG and FZ) served as subjects in this study. All procedures for animal care and experimentation were in accordance with the NIH Guide for the Care & Use of Laboratory Animals (1996) and were approved by our institutional animal experimentation committee. The database used for the present study included 107 neurons that were identical to the sample of neurons in Part 1. All of these neurons showed significant visual responses during the behavioral task, and all of the experimental procedures were the same as those described in Part 1, except for the classification of the neurons.

Recording methods

While the monkeys performed the grouping detection task, we recorded single unit activities from the L-IPS using tungsten microelectrodes that were inserted horizontally into the cortex. Under sodium pentobarbital anesthesia, we implanted an eye coil and placed a head holder and a recording chamber on the skull using standard sterile surgical procedures. Neural signals were amplified and band-pass filtered at 500 Hz to 10 kHz (Nihon Kohden, Tokyo). These signals were then digitalized and recorded on a PC's hard disk at a sampling rate of 25 kHz. After recording, we confirmed the spike activity to be a single neuron using a template-matching method, and then conducted off-line analysis using MATLAB (The MathWorks, Inc.).

Data analysis

Recorded neurons were classified based on action potential duration using the method described previously by Mitchell et al. (2007). We computed the average

waveform of spikes recorded at a sampling rate of 25 kHz. The averaged waveforms were interpolated using a cubic spline function to give a resolution of 2.5 μs. Action potential duration was defined as the time between the trough and the peak of the averaged waveform.

To compare response properties across neuron types classified according to their action potential duration, we first tested the neurons' selectivity for visual features (orientation and contrast) of stimuli composed of multiple dots (see Fig. 14A in Part 1). Firing rates were computed based on the activity recorded within a 200-ms period extending from 50 to 250 ms after stimulus onset. To quantify the selectivity for visual features, we first computed the difference in responses between different target orientations (DBO) and the difference in responses between different target contrasts (DBC) as follows:

DBO = | (WHt + BHt) - (WVt + BVt) | / 2,

DBC = | (WHt + WVt) - (BHt + BVt) | / 2

where WHt, BHt, WVt and BVt respectively represent the response to a target in which white dots are aligned horizontally, black dots are aligned horizontally, white dots are aligned vertically and black dots are aligned vertically. DBO and DBC were separately calculated under each attention condition.

We then quantified the selectivity of each neuron for the target orientation and the target contrast by normalizing the differences between responses to relevant features to the sum of the responses to all features as follows:

Orientation selectivity index = | (WHt + BHt) - (WVt + BVt) | / (WHt + BHt + WVt + BVt)

Contrast selectivity index = | (WHt + WVt) - (BHt + BVt) | / (WHt + BHt + WVt + BVt)

Each selectivity index takes a value between 0 and 1, and a larger value corresponds to stronger selectivity.

To determine the degree to which selectivity was modulated by attention, we calculated a modulation index as follows:

Attention modulation index = (DBOvalid - DBOinvalid) / (DBOvalid + DBOinvalid)

where DBOvalid and DBOinvalid are values of DBO in the valid and invalid conditions, respectively. Modulation indexes ranged between -1 and 1, with a positive value indicating that the selectivity is stronger in the valid condition than the invalid condition.

To examine how the responses to targets differ from those to non-targets, we used rank analysis to compare the responses to the target with those to the non-target. There were 40 stimulus conditions, reflecting 20 stimulus types presented in 2 attended orientations. These stimulus conditions were ranked in the order of the response magnitudes. A stimulus condition ranked 1st was the stimulus condition in which the strongest response was evoked among the 40 stimulus conditions.

Although comparison between correct and error trials would be of interest, the number of error trials for each stimulus was too small to allow systematic analysis. Therefore, except for computing the duration of action potentials, we analyzed only data obtained in correct trials.

Results

Classification of neuron types

We recorded from 107 single neurons in the L-IPS (82 from monkey GG, 25 from monkey FZ). Of those, 94 (71 from monkey GG and 23 from monkey FZ) showed a typical extracellular waveform, with a negative deflection followed by a positive deflection, based upon which we classified these cells as putative pyramidal neurons and interneurons. Figure 14A shows the normalized waveforms of these neurons, while Figure 14B shows the distribution of the action potential durations. Consistent with previous reports, the histogram of action potential durations had two peaks, one at 165 μs and another at 270 μs, and the durations distributed smoothly around these two peaks. We classified neurons with action potential durations shorter than 205 μs (red) as putative interneurons and will refer to them as narrow action potential (Nr) neurons in the following text. Neurons with action potential durations longer than 225 μs (blue) were classified as putative pyramidal neurons and will be referred to as broad action potential (Br) neurons. Neurons with duration between 205 and 225 μs (gray) were excluded from the following analysis because their classification was ambiguous. In addition, to confirm the stability of the action potential durations over recording session, we compared the action potential durations recorded within initial 50 trials and that within last 50 trials. Only two neurons (indicated by white bar) switched the classification, both of which changed from Br classification to Nr classification. We excluded these neurons from the subsequent analysis. After this, about a one-fourth of the neurons were classified as Nr neurons (19 of 65 in monkey GG and 5 of 21 in monkey FZ), and the remaining neurons were classified as Br neurons (46 of 65 neurons in monkey GG

and 16 of 21 in monkey FZ). The average action potential duration was 161.2 ± 27.8 μs (mean ± SD) for the Nr neurons and 295.8 ± 38.5 μs for the Br neurons. In addition, Nr neurons tended to exhibit higher firing rates than Br neurons (Fig. 14C). The average firing rate during the epoch between -150 and 0 ms before stimulus onset was 14.2 ± 10.9 spk/s for Nr neurons and 8.2 ± 7.2 spk/s for Br neurons ($p < 0.05$, Mann-Whitney test; Fig. 14D left), while the average firing rate during stimulus presentation (50-250 ms after stimulus onset) was 28.3 ± 16.2 spk/s for the Nr neurons and 19.6 ± 15.8 spk/s for the Br neurons ($p < 0.05$, Mann-Whitney test; Fig. 14D right). These results are consistent with earlier findings using the same classification scheme and show that putative interneurons tend to exhibit higher activity than putative pyramidal neurons (Diester and Nieder 2008; Johnston et al. 2009; Mitchell et al. 2007). There was no significant difference in the response latencies between Nr neurons (mean ± SD: 63.0 ± 35.4 msec) and Br neurons (73.3 ± 32.7 msec; $p = 0.18$, Mann-Whitney test).

Selective responses to the target orientation: example neuron

To examine the respective contributions made by the two classes of neurons to the visual grouping task, we compared the response properties of Br and Nr neurons. We previously reported that L-IPS neurons exhibit selectivity for the target orientation and that this orientation selectivity was enhanced by attention. Here, we found that there are clear differences between Br and Nr neurons with regard to these response properties.

Figure 15A-C shows the responses of a representive Br neuron displayed as spike density functions. The action potential duration for this neuron was 300 μs. In both the valid (solid line) and invalid (dashed line) conditions, this neuron strongly responded to targets in which dots with the same contrast were aligned vertically (vertical targets),

whereas it did not clearly respond to targets in which dots with the same contrast were aligned horizontally (horizontal targets; Fig. 15A). This preference did not depend on the contrast: similar responses were observed whether the aligned dots were black or white. Although this selectivity was also observed in the invalid condition, responses to the horizontal targets were stronger while those to the vertical targets were weaker, making the orientation selectivity weaker in the invalid condition than in the valid condition.

To quantitatively evaluate target selectivity, we first computed the response magnitudes during the epoch extending from 50 to 250 ms after stimulus onset in each condition (Fig. 15B). We then computed the strength of the selectivity for the orientation and contrast of the target stimuli. In the left panel of Fig. 15C, DBOs (see method) are depicted as vertical bars that correspond to the differences between the mean responses to the horizontal and vertical targets. The black and gray bars depict the DBOs obtained in the valid and invalid conditions, respectively. In the right panel of Fig. 15C, the DBCs depicted correspond to the differences between the mean responses to the white and black targets. The values of DBOs and DBCs were, respectively, 17.1 and 1.7 spk/s in the valid condition and 5.8 and 1.3 spk/s in the invalid condition. DBOs were greater than DBC in both attention conditions, and DBOs were greater in the valid condition than in the invalid condition. This neuron was thus more selective for target orientation than target contrast, and the selectivity for the target orientation was enhanced when the target orientation matched the attended orientation (valid condition). These two characteristics were commonly observed across the population of Br neurons, but not the Nr neurons. Figure 15D-F shows the responses of an example Nr neuron. The responses to the target in which white dots were aligned horizontally was stronger than the responses to other target stimuli (Fig. 15D). However, the selectivity

across the target stimuli was broad (Fig. 15E), so that selectivity for target orientation or target contrast was not clear (Fig. 15F).

Selective responses to the target features: population analysis

To quantify the degree of selectivity for each visual feature, we calculated an orientation selectivity index and a contrast selectivity index for each neuron. In Figure 16, we compare these two indices across the population of L-IPS neurons in the valid (A) and invalid (B) conditions. In Br neurons, the selectivity for the target orientation was greater than for the target contrast (Fig. 16 left column). In the valid condition (Fig. 16A left), a majority of the data points (80.6%; 50 of 62 neurons) were located above the diagonal line, indicating that the orientation selectivity tended to be stronger than the contrast selectivity. As such, the mean orientation selectivity index (0.32) was significantly larger than the mean contrast selectivity index (0.14; $p < 0.001$, Wilcoxon signed-rank test).

The results obtained in the invalid condition are essentially the same as in the valid condition (Fig. 16B left). More than half of the Br neurons (64.5%; 40 of 62 neurons) exhibited greater selectivity for the target orientation than the target contrast, and again the mean orientation selectivity index (0.25) was larger than the mean contrast selectivity index (0.17; $p < 0.01$, Wilcoxon signed-rank test), which is consistent with the results we previously obtained for the entire population of L-IPS neurons (Yokoi and Komatsu 2009).

In contrast to Br neurons, Nr neurons did not exhibit stronger selectivity for the target orientation. In the valid condition (Fig. 16A right), the averages of the orientation and contrast selectivity indexes were 0.12 and 0.09, respectively, while in the invalid

condition (Fig. 16B right) they were 0.15 and 0.13, respectively. There was no significant difference between the orientation and contrast selectivities in either attention condition ($p = 0.35$ in the valid condition, $p > 0.5$ in the invalid condition, Wilcoxon signed-rank test), and the selectivity of Nr neurons for the target orientation was significantly lower than that of Br neurons ($p < 0.05$, Mann-Whitney test). These results indicate that although many neurons in both classes exhibited selectivity for target orientation (Br neuron, 49/62=79.0%, Nr neuron, 15/24=62.5%, ANOVA, $p < 0.05$), the selectivity of Nr neurons was on average much weaker than that of Br neurons. The selectivities for the target contrast were not significantly different between Br and Nr neurons ($p > 0.1$). We also computed the selectivity indexes after subtracting the baseline firing rates. The results were essentially the same as those described in the text.

Effect of attention: population analysis

The example of Br neuron depicted in Fig. 15 showed greater orientation selectivity in the valid condition than in the invalid condition. The effect of attention towards a particular orientation was quantified by computing the attention modulation index for each neuron. The distribution of attention modulation indexes for Br neurons is shown in Fig. 17, left panel. The mean was significantly larger than zero (0.13; $p < 0.05$, one sample Wilcoxon test), indicating that the selectivity for target orientation was greater in the valid condition than in the invalid condition. By contrast, the average attention modulation index in Nr neurons was -0.04, which was not significantly different from zero ($p > 0.5$, one sample Wilcoxon test). These results indicate that Br neurons, on average, have a slight bias towards stronger selectivity in the valid than invalid conditions, but Nr neurons do not.

Nr neurons exhibited higher firing rate than Br neurons (Fig. 14C and D). To confirm that the differences of selectivity and attentional modulation between two classes were not attributable to the difference in the firing rates, we examined the correlation between the firing rates during 50-250 ms after stimulus onset and the orientation selectivities or the absolute value of the attentional modulation indexes. With regard to the orientation selectivity, there tended to be correlation between the firing rate and the orientation selectivity in both Br neurons (r = -0.37, $p < 0.01$) and Nr neurons (r = -0.36, $p = 0.09$). Thus, to examine whether the difference in orientation selectivity between two classes of neurons can be simply explained by the difference in the firing rate, we performed an analysis of covariance (ANCOVA) in which the data from Br neurons and that of Nr neurons were fit with separate lines and it was tested whether the slopes and the intercepts were the same or different. The slope of Br neurons was not significantly different from Nr neurons ($p > 0.05$), whereas the intercept of Br neurons was significantly higher than Nr neurons ($p < 0.05$). This result indicates that the difference in the orientation selectivity cannot be attributable to the difference in firing rate between two classes of neurons. With regard to the attentional modulation, we found that there were no significant correlations between the firing rates and the absolute values of the attention modulation indexes in both Br neurons (r = -0.043, $p > 0.5$) and Nr neurons (r = -0.082, $p > 0.5$).

In the previous part, we have described that responses of L-IPS neurons tended to be enhanced when the monkey directed its attention to a particular orientation for each neuron (Part 1). This can be also seen in the example neurons depicted in Figure 15. The responses of the Br neuron depicted in Fig. 15A-C were enhanced when the monkey directed its attention to the vertical orientation regardless of whether the target

orientation was horizontal (invalid condition) or vertical (valid condition). Similarly, the responses of the Nr neuron depicted in Fig. 15D-F were enhanced when the monkey directed its attention to the horizontal orientation regardless of whether the target orientation was horizontal (valid condition) or vertical (invalid condition). We examined whether this pattern of response modulation is commonly observed in both classes of neurons by comparing the response modulation for the horizontal target and the vertical target. The response modulation was calculated separately for the horizontal and vertical targets. The response modulation for the horizontal target was calculated by subtracting the average of the responses to the horizontal targets when the monkey directed its attention toward the vertical orientation from that when the monkey directed its attention toward the horizontal orientation. The response modulation for the vertical target was calculated in the same manner. Figure 18 compares the response modulations for the horizontal targets (abscissa) and vertical targets (ordinate). If the responses of a given neuron were enhanced when the attention was directed toward a particular orientation regardless of the target orientation, the data point should be plotted within the first- or the third quadrant. We found that this was the case for a large majority of both Br neurons (74.2%; 46 of 62 neurons) and Nr neurons (83.3%; 20 of 24 neurons). These results suggest that the response modulation by attention toward a particular orientation is a common property of both Br neurons and Nr neurons recorded in the present study.

Comparison of the responses to the target and non-target stimuli

A rank analysis carried out in the entire population indicated that the distribution of responses to target stimuli was biased towards the extremes (the smallest and the

largest ranks) due to selectivity for the target orientation (Part 1). In the present study, the results described so far indicate that Br neurons, but not Nr neurons, exhibit such orientation selectivity, which suggests that the distribution of ranks should differ between these two classes of neurons. To test this idea, we conducted separate rank analyses for Br and Nr neurons.

Figure 19 presents the results of rank analyses for the example Br and Nr neurons depicted in Fig. 15. The responses of the Br neuron to the target stimuli showed clear orientation selectivity, and were located at the two extremes of the distribution of responses to non-target stimuli (Fig. 19A). This tendency can be readily seen in Fig. 19B, which shows the ranks of the four target stimuli (white boxes) among the 40 stimuli. The responses to the target stimuli in the valid condition were located near either the top or the bottom of the rank. By contrast, the result of the rank analysis for the example Nr neuron showed a quite different tendency. The responses to the target stimuli tended to be stronger than those to non-target stimuli, and three out of four target stimuli fell above the median for the entire rank (Fig. 19C and D).

These characteristics of the example Br and Nr neurons were commonly observed across the population for each class of neurons. Figure 20 shows the distribution of ranks of the target stimuli for the populations of Br (A) and Nr (B) neurons. The responses of Br neurons were clearly skewed toward both the smallest (strongest response) and largest (weakest response) ranks, and deviated from the uniform distribution (dashed horizontal line). By contrast, the responses of Nr neurons skewed only toward the smallest ranks (strong responses; Fig. 20B), which implies that Nr neurons tend to respond strongly to the target stimuli, regardless of their orientation. In

other words, Nr neurons tend to prefer target over non-target stimuli, but they have little ability to discriminate target orientation.

Discussion

We classified neurons as putative pyramidal neurons (Br neurons) or interneurons (Nr neurons) based on known differences in the extracellular waveforms of their action potentials, and examined the involvement of these two classes of neurons in a visual grouping task. In the following, we will first consider the procedure for classifying neuron types, and then the possible implications of the present results.

In previous studies involving extracellular recording of cortical neurons, narrower action potentials were deemed to have been produced by interneurons, while broader action potentials were from pyramidal neurons (e.g., Mitchell et al. 2007; Rao et al. 1999). This premise was based on intracellular recordings (Connors and Gutnick 1990; Kawaguchi 1993; McCormick et al. 1985) and was further supported by the observed effects of antidromic stimulation of cortical neurons (Johnston et al. 2009). Consistent with several previous studies including a work in the parietal cortex (Maimon and Assad 2009), we found that the distribution of action potential durations was bimodal, and that Nr neurons exhibited higher levels of activity than Br neurons, which suggests that classification of cell types based on action potential duration can be applied to parietal neurons.

We also found that there are clear differences in the response properties of Nr and Br neurons in a visual grouping task. Br neurons showed selectivity for the target orientation, but Nr neurons did not. The orientation selectivity of the responses of Br neurons suggest that these cells encoded visual features of the stimuli, which were comprised of multiple discrete dots. In addition, the orientation selectivity of Br neurons was enhanced when the target orientation matched the attended orientation. Thus the

activities of putative pyramidal neurons were clearly associated with detection of the grouping target.

We found that the proportion of neurons (about 70%) classified as Br neurons across the entire population of cortical neurons was higher than that of Nr neurons, which is consistent with earlier extracellular recordings using the same classification procedure (Diester and Nieder 2008; Johnston et al. 2009; Mitchell et al. 2007). The response properties of Br neurons shown in the present study also matched earlier results analyzed after pooling the entire population of L-IPS neurons (Yokoi and Komatsu 2009), likely because of the large proportion of pyramidal neurons. Our present study clearly indicates that L-IPS neurons signal information about the grouped stimulus to other cortical areas. Regions in the L-IPS are anatomically connected to the inferior temporal (IT) cortex (Blatt et al. 1990; Webster et al. 1994), and the attentional enhancement of signals encoding information about grouped objects may facilitate the object's representation by IT neurons. Pyramidal neurons in the L-IPS may also provide feedback signals and affect the contextual modulation of V1 neurons. The activities of V1 neurons are modulated by the presence of visual stimuli in the receptive field surround, and this contextual modulation is affected by attention (Gilbert et al. 2000). The L-IPS may be an important source of signals related to such contextual modulation.

Putative interneurons (Nr neurons) exhibited weaker orientation selectivity than putative pyramidal neurons (Br neurons), and the orientation selectivity was not enhanced by attention. The function of Nr neurons is not yet clear, but our rank analysis provides some hint as to the possible function of these cells. In contrast to Br neurons, the responses of Nr neurons skewed toward only one extreme (low rank), indicating that the responses to the targets tended to be higher than those to the non-targets. This

suggests three possible functions for these neurons in the current task. First, the activities of Nr neurons may be involved in suppressing the saccade toward the location of the target. It is well established that neurons in the LIP are involved in spatial attention and saccadic eye movements (Balan and Gottlieb 2006; Barash et al. 1991; Bisley and Goldberg 2003, 2006; Colby et al. 1996; Snyder et al. 2000); however, recent evidence shows that LIP neurons are also involved in encoding non-spatial information, such as object shape, color and motion (Freedman and Assad 2006; Janssen et al. 2008; Sereno and Maunsell 1998; Toth and Assad 2002). In the present study, the target stimulus is behaviorally important and draws attention, but monkeys must maintain their eye positions on the fixation spot. Putative interneurons may strongly suppress the activities of the population of LIP neurons involved in making eye movements when the target stimulus appeared, thereby contributing to the performance of the behavioral task, which is mediated using information encoded by the activities of a different population of pyramidal neurons in the same area.

A second possibility is that the activities of putative interneurons modulate the selective responses of Br neurons. We observed that Nr neurons showed broader selectivity than Br neurons, which is similar to earlier observations made in the monkey prefrontal cortex (Constantinidis and Goldman-Rakic 2002; Diester and Nieder 2008). Moreover, studies using multi-channel recording or blockade of GABAergic inhibition suggested that interneurons shape the selectivity of pyramidal neurons (Diester and Nieder 2008; Sato et al. 1996; Tamura et al. 2004; Wang et al. 2000). Although putative interneurons have broad orientation tuning, they may nonetheless contribute to the shaping of selectivity and modulate the orientation selectivity of putative pyramidal neurons.

The third possibility is that interneurons improve the efficiency of signal transmission by pyramidal neurons. It is known that a majority of the neurons exhibiting narrower action potentials are parvalbumin-positive, fast-spiking interneurons (Cauli et al. 1997; Connors and Gutnick 1990; Kawaguchi and Kubota 1997). In addition, recent studies using optogenetics have shown that activation of parvalbumin-positive interneurons induces gamma band oscillation and enhances signal transmission in the cortical microcircuitry (Cardin et al. 2009; Sohal et al. 2009). As will be discussed below, Nr neurons may mediate spatial attention to the target stimulus and improve transmission of target information within the cortical microcircuitry and to other areas.

In an earlier study, Mitchell et al. (2007) showed that putative interneurons are more strongly affected by attention than putative pyramidal neurons in V4. The discrepancy may reflect different involvement of V4 and L-IPS in attention: V4 neurons are affected by attention, whereas neurons in the parietal-frontal network which includes L-IPS are thought to be involved in the allocation of attention. Alternatively, this discrepancy may be explained by the difference in the task design in the two studies. In Mitchell et al.'s study, monkeys were required to allocate attention to the spatial location of the target stimulus. In our study, by contrast, monkeys were required to allocate attention to a particular orientation of a grouped object. As described above, the results of our rank analyses suggested that putative interneurons tend to show stronger responses to the target, which may reflect enhancement of the response to the target when spatial attention was drawn to the target stimulus. If so, it may mean that interneurons in the L-IPS function similarly to those in area V4, and that they are involved in the engagement of spatial attention. Interestingly, fast-spiking interneurons that likely correspond to Nr neurons are involved in the generation of gamma oscillation, which is

thought to be related to spatial attention and its interareal coordination (Fries et al. 2001; Gregoriou et al. 2009). In that context, the activities of Nr neurons in L-IPS and V4 may play similar roles in the allocation of spatial attention to behaviorally important stimuli. By contrast, the principal function of the pyramidal neurons may be to encode visual features, and their activities may be enhanced when attention is directed toward a particular visual feature that is related to the feature selectivity of that pyramidal neuron.

Part 3
Cortico-geniculate feedback linking the visual fields surrounding the blind spot in the cat

Introduction

Classification of L-IPS neurons showed that pyramidal neurons exhibited selectivity for the target stimulus, and clearly indicates that L-IPS neurons signal information about the grouped stimulus to other cortical areas. Neurons in L-IPS may provide feedback signals and affect the activity related to visual grouping in the early visual area. However, no study has explored in detail the feedback projection related to the visual grouping. In an attempt to study the contribution of feedback projection on visual grouping, we examined whether there is an anatomical basis for integration of visual signals from both sides of blind spot (BS) by cortico-geniculate feedback neurons in V1. The blind spot is the region in the visual field that corresponds to the optic disk in the retina. No visual information exists in the blind spot because there are no photoreceptors within the optic disk. Nonetheless, we perceive color and/or patterns there that are the same as in the surrounding visual field. This phenomenon is known as perceptual filling-in, and closely related to the visual grouping. Neural mechanisms under perceptual filling-in at the blind spot has been examined in detail roles (for review, Komatsu 2006), and this provides a good physiological model to investigate the anatomical basis for integration of visual signals related to visual grouping.

The primary visual cortex (V1) is known to send a massive feedback projection to the lateral geniculate nucleus (LGN), but the function of this projection remains largely unknown. Notably, the axons of V1 neurons projecting back to the LGN show broad

arborization, spanning 0.5-1.5 mm (Murphy and Sillito 1996), which is much larger than the arborization of feedforward projections from retinal ganglion cells to the LGN (Bowling and Michael 1984). This suggests that feedback from V1 to the LGN may be involved in the integration or interaction of visual information present from separate locations within the visual field.

The blind spot of the cat is oval in shape, extending 5 to 6 deg in the major axis, and is located at about the retinotopic coordinate of (azimuth=14.6 deg, elevation =6.5deg) relative to the area centralis in the temporal hemi-field (Bishop et al. 1962). This means that when perceptual filling-in occurs at the blind spot, neural signals carrying the visual attributes of the region surrounding the blind spot must be integrated across the large gap in the visual field that corresponds to the blind spot. Possible neural substrates for the spatial integration of visual signals involving V1 and relating to perceptual filling-in include horizontal connections within V1, feedback from the extrastriate cortex to V1 and the feedback projection from V1 to the LGN (Matsumoto and Komatsu 2005).

Previous studies showed that when perceptual filling-in or completion occurs at the blind spot, mainly neurons in and around the region of V1 that retinotopically corresponds to the blind spot (blind spot region) in layer 6 are activated (Komatsu et al. 2000; Matsumoto and Komatsu 2005). One of the main targets of layer 6 neurons is the LGN, which suggests that the neural mechanisms underlying perceptual filling-in involve the feedback projection from V1 to the LGN (Komatsu et al. 2002). Furthermore, if feedback to the LGN is responsible for the integration of visual signals across the blind spot, we can assume that axons from layer 6 neurons situated at one side of the blind spot region send fibers to both sides of the blind spot region in the LGN, thereby

enabling the integration of visual information across the blind spot at the level of LGN. However, no study has explored in detail the feedback projection from V1 to the blind spot region of the LGN. Within the LGN, visual information from the right and left eyes is separated into different layers. Consequently, there is a neuron-free gap in the LGN layer receiving visual input from the contralateral eye corresponding to the blind spot of that eye. For example, there is a gap in a specific layer of the LGN in the left hemisphere that corresponds to the right eye's blind spot.

In this experiment, we examined whether feedback axon fibers from neurons located around the blind spot region in V1 traverse the gap in the LGN corresponding to the blind spot of a cat. Cats have a blind spot similar in size to that of the monkey and, for study, they have an advantage over monkeys in that the structure of their LGN is relatively simple (3 main layers in the cat LGN vs. 6 main layers in the monkey LGN), and the gap corresponding to the blind spot can be easily identified in histological sections (Kaas et al. 1973). Of the three main layers in the LGN of the cat (layers A, A1 and C from dorsal to ventral), layer A receives inputs from the contralateral eye and contains the neuron-free gap corresponding to the blind spot. We found that axon fibers from V1 traverse this gap within the LGN and are capable of integrating visual signals from both sides of the blind spot.

Materials and methods

BDA injection and visualization

A cat weighing 2.85 kg was used for the experiment. General anesthesia was induced with ketamine hydrochloride (7.5 mg/kg i.m.) and medetomizine hydrochrolide (0.06 mg/kg i.m.), after which the cat was intubated and artificially ventilated, and anesthesia was maintained with 0.5-3.0 % of isoflurane in a 1:1 mixture with N2O-O2. In addition, the cat was paralyzed with pancronium bromide (0.1 mg/kg/h i.v.; Mioblock, Sankyou, Tokyo). Then using standard sterile technique, a recording chamber was attached over the skull with dental acrylic. The recording chamber was placed on the postero-dorsal surface above V1.

We recorded neuronal activity from V1 in the right hemisphere using tungsten microelectrodes (Frederic Haer). We initially presented visual stimuli (bar or spot) on a tangent screen and mapped the receptive fields (RFs) of V1 neurons. By using occluding masks, we were able to present the stimuli to either the right or left eye separately. Moreover, by projecting the optic disk of the left eye onto the tangent screen (Cooper ML and Pettigrew 1979), we were able to identify the V1 region representing the blind spot by mapping the RFs across the V1 surface. Electrodes were vertically penetrated at five different sites separated by 1 mm each in the posterior part of V1. In each penetration, after passing through the lateral surface of V1 and white matter, we encountered V1 cortex again where the receptive field center gradually shifted toward more peripheral and upper visual field from about 8-10 deg in azimuth to 15-18 deg as the electrode was advanced. At one site, the receptive field center shifted from (azimuth = 10 deg, elevation = 3 deg) gradually toward inside of the visual field corresponding to

the blind spot.

After identifying the blind spot region in V1, we inserted a glass micropipette (tip diameter, 25 μm) filled with 10% biotinylated dextran amine (BDA, 3000 molecular weight, Molecular Probes) in 0.01 M phosphate butter (PB) into a location adjacent to the blind spot region in V1. At a level 5950 μm from the V1 surface, we injected BDA by iontophoresis (positive-pulsed DC current 7.0 μA, 7 s on and 7 s off for 20 min) and then continued to hold the tip of the micropipette at the same depth for 5 min after the injection was finished. Figure 21a schematically illustrates the experimental design.

Fifteen days after the BDA injection, the cat was deeply anesthetized with sodium pentobarbital and then perfused via the heart with 0.1 M phosphate-buffered saline (PBS) and 4% paraformaldehyde in 0.1 M PB. The brain was then removed from the skull, and using a cryostat (CM3050, Leica, Germany), serial coronal sections (50 μm thick) were cut from a tissue block containing the LGN from the right hemisphere and placed in 0.1 M PBS. To visualize the BDA-stained axon fibers, a series of sections was incubated for 2 h at room temperature in a solution of avidin-biotin complex (Vectastain Elite ABC kit, Vector) also containing 0.4% Triton X-100 (TX-100, Sigma). After rinsing first in 0.1 M PBS and then in 0.05 M Tris-buffered saline (TBS), the sections were preincubated in 0.05 M TBS containing 0.02% diaminobenzidine hydrochloride (DAB, Sigma) and 0.07% nickel(II) chloride hexahydrate, and then incubated in another DAB solution containing 0.003% hydrogen peroxide. The reaction time was adjusted to optimize the contrast of the label, after which the sections were rinsed in 0.05 M TBS and 0.1 M PBS to terminate the reaction. The sections were then mounted onto gelatin-coated slides, dried and coverslipped. After all the axon tracing around the neuron-free gap has been finished in sections without counter-staining, we removed the

cover glass of the sections and stained sections with cresyl violet for the reconstruction of the entire LGN. We also stained V1 sections around the injection site with cresyl violet. BDA injection site in V1 was identified histologically in the deep layers of V1 at the fundus of the suprasplenial suclus about 500 μm in size measured as the diameter of the dense core excluding the hallo. We have estimated the retinotopic position of the BDA injection based on the histological reconstruction of LGN. By comparing the positions of the neuron-free gap corresponding to the optic disk and the focus of projection in LGN, we estimated the retinotopic position of the injection site referring to the retinotopic map of LGN reported previously (Sanderson 1971a).

All procedures related to animal care and experiments were in accordance with the National Institutes of Health Guide for the Care and Use of Laboratory Animals (1996) and were approved by our institutional animal experimentation committee.

Results

Feedback projection traversing the blind spot in LGN

When we inspected the Nissl-stained sections under a microscope, a neuron-free gap spanning about 100 μm was clearly visible in layer A (Fig. 21b). No such gap was observed in layer A1. LGN of the cat has upward curving in the posterior part and the neuron-free gap corresponding to the optic disk is located at the anterior-posterior level where the upward curving of the LGN starts to occur (Guillery and Kaas 1971). Our reconstruction of LGN indicates that the coronal level of the section in Fig. 21b roughly corresponds to the upward curving of LGN. In addition, we did not observe any clear neuron-free gap in other part of LGN. These results provide converging evidence that the neuron-free gap in Fig. 21b corresponds to the representation of the optic disk.

The BDA-labeled axons were distributed in a columnar fashion in the serial sections, and in the section containing the neuron-free gap, a dense patch of BDA-labeled axon terminals was observed approximately 500 μm medial from the gap (Fig. 21b arrow). We estimated the retinotopic position of the injection site referring to the retinotopic map of LGN reported previously by comparing the positions of the gap corresponding to the optic disk and the focus of projection in LGN. The coronal level of the center of the neuron-free gap as shown in Fig. 21b corresponds to 2.9/10 of the entire length of the LGN measured from the posterior pole forwards that is the same coordinate as that used by Sanderson (1971a). Judging from the retinotopic map in Fig. 3 of his paper, the retinotopic position of the injected site should be about (azimuth=10 deg, elevation=1.5deg). The estimate based on the magnification factor in LGN (Sanderson 1971b) gives a similar retinotopic position.

We examined the labeled axon fibers emanating from the dense patch toward the neuron-free gap in layer A in sections without counter-staining. Using differential interference contrast (Nomarski) microscopy, we were able to clearly identify the neuron-free gap in layer A, even in sections without counter-staining. The gap is indicated as the region between the asterisks in Fig. 1c. In these sections, we observed numerous axon fibers traversing from the medial side of the gap toward the lateral side, and the photomicrograph in Fig. 1c contains an example of one such axon fiber (black arrow).

Figure 21d was constructed from 10 sections and shows axon fibers terminating at the lateral side of the gap, opposite the dense patch of axons. It can be seen that many axon fibers traverse the gap corresponding to the blind spot, and that these fibers contain numerous boutons, suggesting the presence of synapses in both sides of the gap. Taken together, these results indicate that a feedback signal from a single V1 neuron can affect multiple LGN neurons situated on both sides of the gap that have RFs on opposite sides of the blind spot and are separated at least 5 to 6 deg in the visual field.

Discussion

In the present study, the maximum spread of axons from the densely labeled zone was about 700 μm, which is well within the spread previously reported for some axons (Murphy and Sillito 1996). Labeled axons traversed the neuron-free gap in the LGN corresponding to the blind spot, and synaptic boutons were observed on both sides of the gap. This suggests that cortico-geniculate axons form synaptic connections with LGN neurons having RFs in the visual fields more central and more peripheral than the blind spot. Moreover, several synaptic boutons were observed within the gap (Fig. 21d); presumably, dendrites of LGN neurons situated around the gap encroach into the gap and make contact with the cortico-geniculate axons there. Several studies have reported that inactivation of cortico-geniculate feedback reduces the influence of stimuli presented outside the RF (e.g., Murphy and Sillito 1987; Rivadulla et al. 2002), which suggests that visual signals from RF surrounds are integrated via the cortico-geniculate feedback pathway. It is suggested that cortico-geniculate feedback shifts the balance of mechanisms underlying the centre-surround organization of the receptive fields, and promote both segmentation and integration of contours (Sillito and Jones 2002). This modulatory influence of cortico-geniculate feedback is thought to be exerted in a feature-selective manner (Murphy et al. 1999). In addition, some cortico-geniculate neurons in layer 6 of V1 show marked spatial summation (Gilbert 1977; Tsumoto and Suda 1980) although it is also reported that most cortico-geniculate neurons have small receptive field (Grieve and Sillito 1995). The properties enabling feature-specific modulatory influence are well suited for linking specific features present around the blind spot and mediating the filling-in of color/brightness or completion of contours. It

has been shown that at least some of the cortico-geniculate neurons in V1 are binocularly driven (Gilbert 1977; Grieve and Sillito 1995) and that their axons innervate both layers A and A1 in the LGN (Robson 1983). This suggests cortico-geniculate projections may play an important role in the interocular transfer of visual signals. Thus the filling-in at the blind spot, which has been shown to exhibit interocular transfer (Murakami 1995), may be mediated by this feedback projection.

Cortico-geniculate feedback exerts a modulatory effect on LGN activities in a variety of ways, including gain modulation (Tsumoto et al. 1978), changes in firing mode (Sherman and Guillery 2001; Wang et al. 2006) and synchronization of the spike firing of separate LGN neurons (Sillito et al. 1994), and one or more of these may also be involved in the filling-in or completion at the blind spot.

Our present results suggest that one possible mechanism of perceptual filling-in at the blind spot is the integration of visual signals from around the blind spot through feedback and feedforward looping between V1 and the LGN. These findings may also provide new insight into the possible role of the massive feedback projection from V1 to the LGN.

General conclusion

We recorded neuronal activities in L-IPS while monkeys performed a grouping detection task. We found that L-IPS neurons selectively responded to target orientation, that this selectivity was enhanced when the target orientation matched the attended orientation, and that the orientation-selective responses correlated with the monkeys' behavior. In the experiment of classification of neuron type, we found that putative pyramidal neurons in L-IPS exhibited selectivity for the orientation of the target, and this selectivity was enhanced by attention to a particular target orientation. This result indicates that L-IPS neurons signal information about the grouped stimulus to other cortical areas. In the anatomical experiment, we found the feedback connection linking the visual fields surrounding the blind spot, which may be involved in the integration or interaction of visual information present from separate locations within the visual field. Neuronal activity in V1 is modulated by the presentation of visual stimuli in the receptive field surround, and it has been suggested that this contextual modulation is related to the visual grouping (Gilbert et al., 2000). Presumably, L-IPS neurons provide feedback signals to the early visual areas and facilitate visual grouping by way of the contextual modulation there.

These results provide the first physiological evidence that L-IPS neurons make an important contribution to visual grouping by combining visual and attentional signals to bind discrete visual elements. A recurrent circuit between the L-IPS and early visual areas may be critical for visual grouping through the interchange of feedforward and feedback signals.

Acknowledgements

I would like to express sincere gratitude to all people who helped me during the experiment. I deeply appreciate Prof. H. Komatsu for his supervision and suggestion thorough the experiment. I thank members at Division of Sensory and Cognitive Information; M.Ito, K.Koida, N.Goda, C.Hiramatsu, T.Ogawa for helpful discussions and suggestions during the course of study; many graduate students for their valuable time and energy to help me perform experiments. I would also like to extend my gratitude to all laboratory members. This experiment would not be possible without technical supports by M.Togawa, R.Hirokawa, T.Ohta, M.Ohba, N.Takahashi and M.Takagi. They provided tremendous supports throughout the experiment.

I also thank Y. Wang and Y. Kawaguchi for their expert advice.

I must appreciate the understanding of my family, RY, TY and YY. They provided time of rest and relaxation.

Finally I would like to thank Prof. Hidehiko Komatsu. Thank you *so* much for giving me time, passion and encouragement.

References

Balan PF, Gottlieb J (2006) Integration of exogenous input into a dynamic salience map revealed by perturbing attention. *J Neurosci* 26:9239-9249.

Barash S, Bracewell RM, Fogassi L, Gnadt JW, Andersen RA (1991) Saccade-related activity in the lateral intraparietal area. I. Temporal properties; comparison with area 7a. *J Neurophysiol* 66:1095-1108.

Ben Hamed S, Duhamel JR, Bremmer F, Graf W (2001) Representation of the visual field in the lateral intraparietal area of macaque monkeys: a quantitative receptive field analysis. *Exp Brain Res* 140:127-144.

Bishop PO, Kozak W, Vakkur GJ (1962) Some quantitative aspects of the cat's eye: axis and plane of reference, visual field co-ordinates and optics. *J Physiol* 163:466-502

Bisley JW, Goldberg ME (2003) Neuronal activity in the lateral intraparietal area and spatial attention. *Science* 299:81-86.

Bisley JW, Krishna BS, Goldberg ME (2004) A rapid and precise on-response in posterior parietal cortex. *J Neurosci* 24:1833-1838.

Bisley JW, Goldberg ME (2006) Neural correlates of attention and distractibility in the lateral intraparietal area. *J Neurophysiol* 95:1696-1717.

Blatt GJ, Andersen RA, Stoner GR (1990) Visual receptive field organization and cortico-cortical connections of the lateral intraparietal area (area LIP) in the macaque. *J Comp Neurol* 299:421-445.

Borra E, Belmalih A, Calzavara R, Gerbella M, Murata A, Rozzi S, Luppino G (2008) Cortical connections of the macaque anterior intraparietal (AIP) area. *Cereb Cortex* 18:1094-1111.

Bowling DB, Michael CR (1984) Terminal patterns of single, physiologically characterized optic tract fibers in the cat's lateral geniculate nucleus. *J Neurosci* 4:198-216

Cardin JA, Carlen M, Meletis K, Knoblich U, Zhang F, Deisseroth K, Tsai LH, Moore CI (2009) Driving fast-spiking cells induces gamma rhythm and controls sensory responses. *Nature* 459:663-667.

Cauli B, Audinat E, Lambolez B, Angulo MC, Ropert N, Tsuzuki K, Hestrin S, Rossier J (1997) Molecular and physiological diversity of cortical nonpyramidal cells. *J Neurosci* 17:3894-3906.

Colby CL, Duhamel JR, Goldberg ME (1996) Visual, presaccadic, and cognitive activation of single neurons in monkey lateral intraparietal area. *J Neurophysiol* 76:2841-2852.

Connors BW, Gutnick MJ (1990) Intrinsic firing patterns of diverse neocortical neurons. *Trends Neurosci* 13:99-104.

Connor CE, Brincat SL, Pasupathy A (2007) Transformation of shape information in the ventral pathway. *Curr Opin Neurobiol* 17:140-147.

Constantinidis C, Goldman-Rakic PS (2002) Correlated discharges among putative pyramidal neurons and interneurons in the primate prefrontal cortex. *J Neurophysiol* 88:3487-3497.

Cooper ML, Pettigrew JD (1979) A neurophysiological determination of the vertical horopter in the cat and owl. *J Comp Neurol* 184:1-26

Coslett HB, Saffran E (1991) Simultanagnosia. To see but not two see. *Brain* 114:1523-1545.

Desimone R, Albright TD, Gross CG, Bruce C (1984) Stimulus-selective properties of inferior temporal neurons in the macaque. *J Neurosci* 4:2051-2062.

Desimone R, Duncan J (1995) Neural mechanisms of selective visual attention. *Annu Rev Neurosci* 18:193-222.

Desimone R, Schein SJ (1987) Visual properties of neurons in area V4 of the macaque: sensitivity to stimulus form. *J Neurophysiol* 57:835-868.

Diester I, Nieder A (2008) Complementary contributions of prefrontal neuron classes in abstract numerical categorization. *J Neurosci* 28:7737-7747.

Durand JB, Nelissen K, Joly O, Wardak C, Todd JT, Norman JF, Janssen P, Vanduffel W, Orban GA (2007) Anterior regions of monkey parietal cortex process visual 3D shape. *Neuron* 55:493-505.

Fink GR, Halligan PW, Marshall JC, Frith CD, Frackowiak RS, Dolan RJ (1996) Where in the brain does visual attention select the forest and the trees? *Nature* 382:626-628.

Freedman DJ, Assad JA (2006) Experience-dependent representation of visual categories in parietal cortex. *Nature* 443:85-88.

Friedman-Hill SR, Robertson LC, Treisman A (1995) Parietal contributions to visual feature binding: evidence from a patient with bilateral lesions. *Science* 269:853-855.

Fries P, Reynolds JH, Rorie AE, Desimone R (2001) Modulation of oscillatory neuronal synchronization by selective visual attention. *Science* 291:1560-1563.

Gattass R, Gross CG, Sandell JH (1981) Visual topography of V2 in the macaque. *J Comp Neurol* 201:519-539.

Gattass R, Sousa AP, Gross CG (1988) Visuotopic organization and extent of V3 and V4 of the macaque. *J Neurosci* 8:1831-1845.

Gilbert C, Ito M, Kapadia M, Westheimer G (2000) Interactions between attention, context and learning in primary visual cortex. *Vision Res* 40:1217-1226.

Gnadt JW, Andersen RA (1988) Memory related motor planning activity in posterior parietal cortex of macaque. *Exp Brain Res* 70:216-220.

Grefkes C, Fink GR (2005) The functional organization of the intraparietal sulcus in humans and monkeys. *J Anat* 207:3-17.

Gregoriou GG, Gotts SJ, Zhou H, Desimone R (2009) High-frequency, long-range coupling between prefrontal and visual cortex during attention. *Science* 324:1207-1210.

Heinze HJ, Hinrichs H, Scholz M, Burchert W, Mangun GR (1998) Neural mechanisms of global and local processing. A combined PET and ERP study. *J Cogn Neurosci* 10:485-498.

Himmelbach M, Erb M, Klockgether T, Moskau S, Karnath HO (2009) fMRI of global visual perception in simultanagnosia. *Neuropsychologia* 47:1173-1177.

Janssen P, Srivastava S, Ombelet S, Orban GA (2008) Coding of shape and position in macaque lateral intraparietal area. *J Neurosci* 28:6679-6690.

Johnston K, Everling S (2006) Monkey dorsolateral prefrontal cortex sends task-selective signals directly to the superior colliculus. *J Neurosci* 26:12471-12478.

Judge SJ, Richmond BJ, Chu FC (1980) Implantation of magnetic search coils for measurement of eye position: an improved method. *Vision Res* 20:535-538.

Kaas JH, Guillery RW, Allman JM (1973) Discontinuities in the dorsal lateral geniculate nucleus corresponding to the optic disc: a comparative study. *J Comp Neurol* 147:163-179

Kawaguchi Y (1993) Groupings of nonpyramidal and pyramidal cells with specific physiological and morphological characteristics in rat frontal cortex. *J Neurophysiol* 69:416-431.

Kawaguchi Y, Kubota Y (1997) GABAergic cell subtypes and their synaptic connections in rat frontal cortex. *Cereb Cortex* 7:476-486.

Komatsu H (2006) The neural mechanisms of perceptual filling-in. *Nat Rev Neurosci* 7:220-231

Komatsu H, Kinoshita M, Murakami I (2000) Neural responses in the retinotopic representation of the blind spot in the macaque V1 to stimuli for perceptual filling-in. *J Neurosci* 20:9310-9319

Komatsu H, Kinoshita M, Murakami I (2002) Neural responses in the primary visual cortex of the monkey during perceptual filling-in at the blind spot. *Neurosci Res* 44:231-236

Lehky SR, Sereno AB (2007) Comparison of shape encoding in primate dorsal and ventral visual pathways. *J Neurophysiol* 97:307-319.

Lewis JW, Van Essen DC (2000) Mapping of architectonic subdivisions in the macaque monkey, with emphasis on parieto-occipital cortex. *J Comp Neurol* 428:79-111.

Maimon G, Assad JA (2009) Beyond Poisson: increased spike-time regularity across primate parietal cortex. *Neuron* 62:426-440.

Matsumoto M, Komatsu H (2005) Neural responses in the macaque v1 to bar stimuli with various lengths presented on the blind spot. *J Neurophysiol* 93:2374-2387

McCormick DA, Connors BW, Lighthall JW, Prince DA (1985) Comparative electrophysiology of pyramidal and sparsely spiny stellate neurons of the neocortex. *J Neurophysiol* 54:782-806.

Mitchell JF, Sundberg KA, Reynolds JH (2007) Differential attention-dependent response modulation across cell classes in macaque visual area V4. *Neuron* 55:131-141.

Murakami I (1995) Motion aftereffect after monocular adaptation to filled-in motion at the blind spot. *Vision Res* 35:1041-1045

Murata A, Gallese V, Luppino G, Kaseda M, Sakata H (2000) Selectivity for the shape, size, and orientation of objects for grasping in neurons of monkey parietal area AIP. *J Neurophysiol* 83:2580-2601.

Murphy PC, Duckett SG, Sillito AM (1999) Feedback connections to the lateral geniculate nucleus and cortical response properties. *Science* 286:1552-1554

Murphy PC, Sillito AM (1987) Corticofugal feedback influences the generation of length tuning in the visual pathway. *Nature* 329:727-729

Murphy PC, Sillito AM (1996) Functional morphology of the feedback pathway from area 17 of the cat visual cortex to the lateral geniculate nucleus. *J Neurosci* 16:1180-1192

Navon D (1977) Forest before trees: the precedence of global features in visual perception. *Cogn Psychol* 9:353–383.

Palmer SE (1999) Organizing objects and scenes. In: *Vision science*: Photons to phenomenology (Palmer SE, ed), pp254-310. Cambridge, MA: MIT.

Pasupathy A, Connor CE (2002) Population coding of shape in area V4. *Nat Neurosci* 5:1332-1338.

Rao SG, Williams GV, Goldman-Rakic PS (1999) Isodirectional tuning of adjacent interneurons and pyramidal cells during working memory: evidence for microcolumnar organization in PFC. *J Neurophysiol* 81:1903-1916.

Reynolds JH, Desimone R (2003) Interacting roles of attention and visual salience in V4. *Neuron* 37:853-863.

Rivadulla C, Martinez LM, Varela C, Cudeiro J (2002) Completing the corticofugal loop: a visual role for the corticogeniculate type 1 metabotropic glutamate receptor. *J*

Neurosci 22:2956-2962

Robertson LC, Lamb MR, Knight RT (1988) Effects of lesions of temporal-parietal junction on perceptual and attentional processing in humans. *J Neurosci* 8:3757-3769.

Robinson DA (1963) A method of measuring eye movement using a scleral search coil in a magnetic field. *IEEE Trans Biomed Eng* 10:137-145.

Robson JA (1983) The morphology of corticofugal axons to the dorsal lateral geniculate nucleus in the cat. *J Comp Neurol* 216:89-103

Sanderson KJ (1971a) The projection of the visual field to the lateral geniculate and medial interlaminar nuclei in the cat. *J Comp Neurol* 143:101-108

Sanderson KJ (1971b) Visual field projection columns and magnification factors in the lateral geniculate nucleus of the cat. *Exp Brain Res* 13:159-177

Sasaki Y, Hadjikhani N, Fischl B, Liu AK, Marrett S, Dale AM, Tootell RB (2001) Local and global attention are mapped retinotopically in human occipital cortex. *Proc Natl Acad Sci U S A.* 98:2077-2082.

Sato H, Katsuyama N, Tamura H, Hata Y, Tsumoto T (1996) Mechanisms underlying orientation selectivity of neurons in the primary visual cortex of the macaque. *J Physiol* 494 (Pt 3):757-771.

Sereno AB, Amador SC (2006) Attention and memory-related responses of neurons in the lateral intraparietal area during spatial and shape-delayed match-to-sample tasks. *J Neurophysiol* 95:1078-1098.

Sereno AB, Maunsell JH (1998) Shape selectivity in primate lateral intraparietal cortex. *Nature* 395:500-503.

Shadlen MN, Newsome WT (2001) Neural basis of a perceptual decision in the parietal cortex (area LIP) of the rhesus monkey. *J Neurophysiol* 86:1916-1936.

Sherman SM, Guillery RW (2001) Exploring the thalamus. Academic Press, San Diego

Sillito AM, Jones HE (2002) Corticothalamic interactions in the transfer of visual information. *Philos Trans R Soc Lond B Biol Sci* 357:1739-1752

Sillito AM, Jones HE, Gerstein GL, West DC (1994) Feature-linked synchronization of thalamic relay cell firing induced by feedback from the visual cortex. *Nature* 369:479-482

Snyder LH, Batista AP, Andersen RA (2000) Intention-related activity in the posterior parietal cortex: a review. *Vision Res* 40:1433-1441.

Sohal VS, Zhang F, Yizhar O, Deisseroth K (2009) Parvalbumin neurons and gamma rhythms enhance cortical circuit performance. *Nature* 459:698-702.

Taira M, Mine S, Georgopoulos AP, Murata A, Sakata H (1990) Parietal cortex neurons

of the monkey related to the visual guidance of hand movement. *Exp Brain Res* 83:29-36.

Tamura H, Kaneko H, Kawasaki K, Fujita I (2004) Presumed inhibitory neurons in the macaque inferior temporal cortex: visual response properties and functional interactions with adjacent neurons. *J Neurophysiol* 91:2782-2796.

Tanaka H, Onoe H, Tsukada H, Fujita I (2001) Attentional modulation of neural activity in the macaque inferior temporal cortex during global and local processing. *Neurosci Res* 39:469-472.

Tanaka K, Saito H, Fukada Y, Moriya M (1991) Coding visual images of objects in the inferotemporal cortex of the macaque monkey. *J Neurophysiol* 66:170-189.

Toth LJ, Assad JA (2002) Dynamic coding of behaviourally relevant stimuli in parietal cortex. *Nature* 415:165-168.

Tsumoto T, Creutzfeldt OD, Legendy CR (1978) Functional organization of the corticofugal system from visual cortex to lateral geniculate nucleus in the cat (with an appendix on geniculo-cortical mono-synaptic connections). *Exp Brain Res* 32:345-364

Tsumoto T, Suda K (1980) Three groups of cortico-geniculate neurons and their distribution in binocular and monocular segments of cat striate cortex. *J Comp Neurol* 193:223-236

Wang W, Jones HE, Andolina IM, Salt TE, Sillito AM (2006) Functional alignment of feedback effects from visual cortex to thalamus. *Nat Neurosci* 9:1330-1336

Wang Y, Fujita I, Murayama Y (2000) Neuronal mechanisms of selectivity for object features revealed by blocking inhibition in inferotemporal cortex. *Nat Neurosci* 3:807-813.

Warrington EK, James M (1967) Disorders of visual perception in patients with localised cerebral lesions. *Neuropsychologia* 5:253-266.

Webster MJ, Bachevalier J, Ungerleider LG (1994) Connections of inferior temporal areas TEO and TE with parietal and frontal cortex in macaque monkeys. *Cereb Cortex* 4:470-483.

Wertheimer M (1950) Laws of organization in perceptual forms. In: *A sourcebook of Gestalt psychology* (Ellis WD, ed), pp71-81. New York: The Humanities Press (Original work published 1923).

Xu Y, Chun MM (2007) Visual grouping in human parietal cortex. *Proc Natl Acad Sci USA* 104:18766-18771.

Xu Y (2008) Representing connected and disconnected shapes in human inferior intraparietal sulcus. *Neuroimage* 40:1849-1856.

Figures

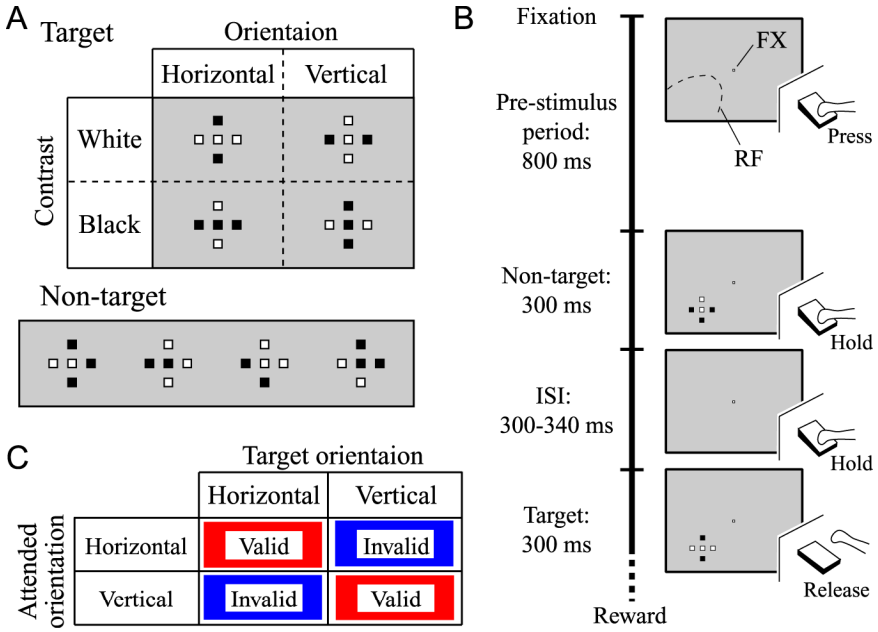

Figure 1 Visual stimuli and sequence of the grouping detection task.
A: Twenty types of visual stimuli (four targets and sixteen non-targets) were used. Each was composed of five square black or white dots arranged in a cross. Target stimuli were arranged so that dots with the same contrast were aligned horizontally or vertically (top panel), and were characterized by two features: orientation and contrast. Other arrangements were used as non-target stimuli, four of which are shown in the bottom panel. Note that the contour line of the dot is for illustration purposes only and was not present in the actual stimulus in the experiment.
B: Time course of a trial. During a trial, while the monkey maintained fixation, visual stimuli were presented serially up to 3 (or 4) times within the receptive field (RF). The monkey was required to quickly release the lever when the target was presented. FX is the fixation spot.
C: Relationship matrix between the target orientation and the attended orientation. In the valid condition, the target orientation matched the attended orientation. In the invalid condition, the target orientation was orthogonal to the attended orientation.

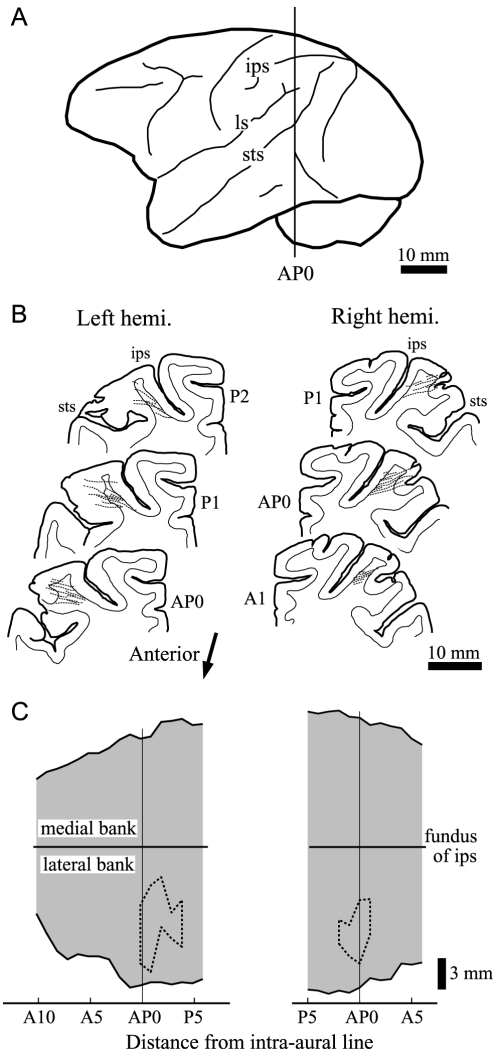

Figure 2

Histological reconstruction of the recording sites in one monkey (GG).

Brain slices were examined microscopically and drawn by using a camera lucida. Histologically identified electrode tracks are superimposed on the nearest representative slices at 1 mm intervals. Electrode tracks were densely distributed in the middle portion of the lateral bank of the intraparietal sulcus (L-IPS) (left hemisphere: A0-P4, right hemisphere: A1-P2).

A: Side view of the brain; the vertical line indicates the intra-aural line (AP0).

B: Coronal sections showing the recording sites. Dotted lines indicate histologically identified electrode tracks projected on the nearest section at 1-mm interval.

C: Location of the recording sites on the flattened intraparietal sulcus. The regions surrounded by the dotted lines represent the recording sites identified by histological reconstruction and are located in the L-IPS. Right and left panels correspond to the right and left hemispheres, respectively. ips: intraparietal sulcus, ls: lateral sulcus, sts: superior temporal sulcus.

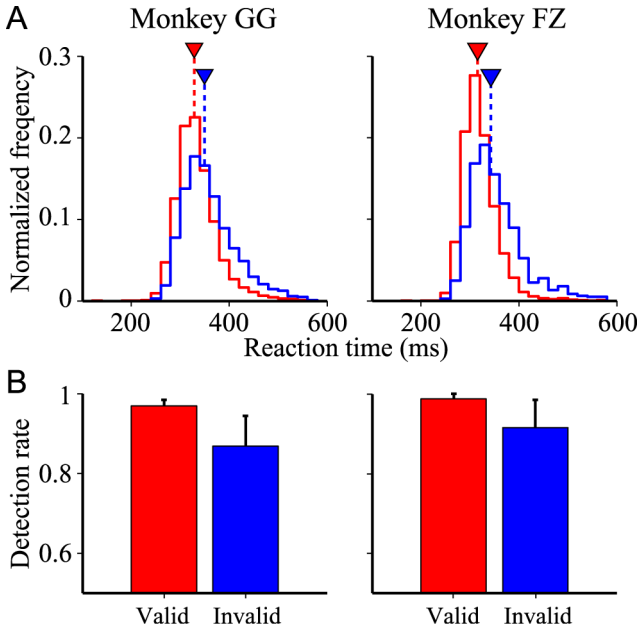

Figure 3 Performance of the behavioral task and the effect of attention.
Left and right panels illustrate the results of monkeys GG and FZ, respectively.
A: Distribution of the reaction times in the valid (red) and invalid (blue) conditions. The triangles indicate the mean reaction times.
B: Average detection rate across the neuronal recording sessions. Error bars indicate the standard deviation (SD).

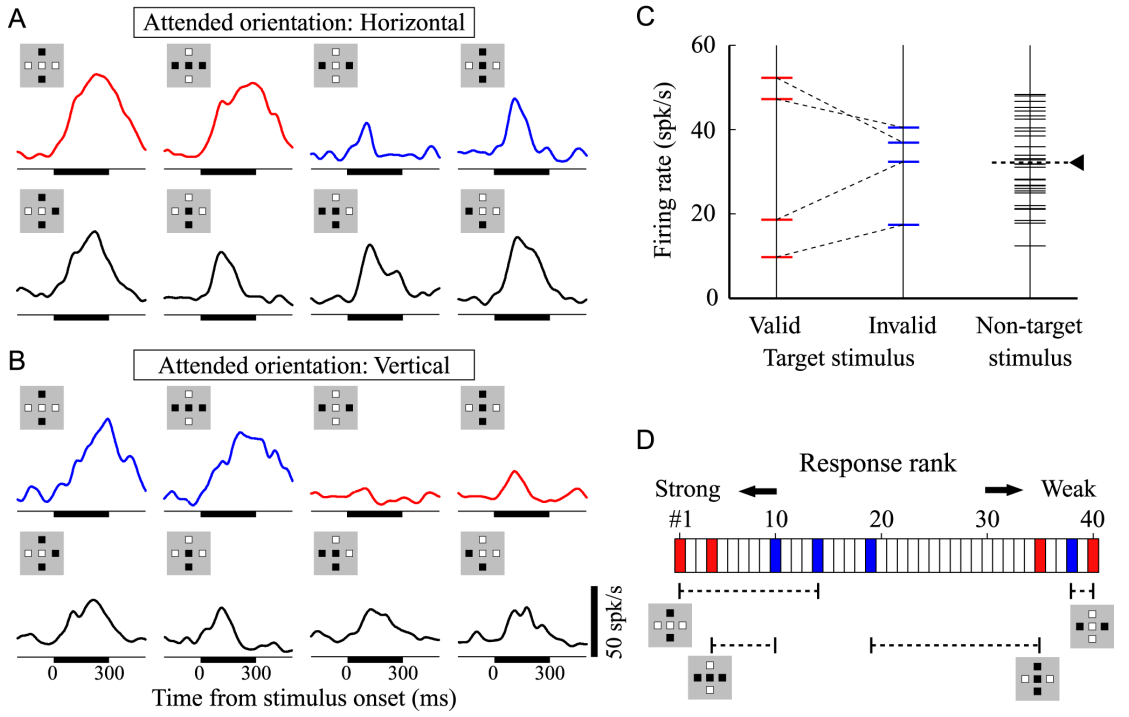

Figure 4 Responses of an example L-IPS neuron to the target and non-target stimuli.
A: Responses to the target (top row) and non-target (bottom row) stimuli when the monkey attended to the horizontal orientation. Responses are shown as spike density functions, which were obtained by convolving the spike train (resolution of 1 ms) with a Gaussian kernel (SD=20 ms). Thick horizontal bars on the bottom indicate the stimulus presentation periods. In this and other panels, red (blue) represents the valid (invalid) condition.
B: Responses to visual stimuli when the monkey attended to the vertical orientation. Other explanations are the same as in A.
C: Responses to all stimuli in both attention conditions. Each stimulus in each attention condition corresponds to a horizontal bar, and the firing rate elicited by each stimulus is indicated by the height of the bar. In the leftmost column depicts responses to target stimuli in the valid condition (red), the middle column the invalid condition (blue). Dotted lines connect the responses to the same target stimulus. The rightmost column depicts responses to non-target stimuli. A triangle and broken line represents the average of the responses to non-target stimuli.
D: Ranking of the responses to the target stimuli across the four targets among the 40 stimuli. Red and blue bars indicate the ranks of the responses to the targets illustrated below. Ranks of the responses to the same targets are connected by dashed lines. White bars represent the ranks of non-targets. The stimulus that induced the strongest response is ranked #1 and the weakest #40.

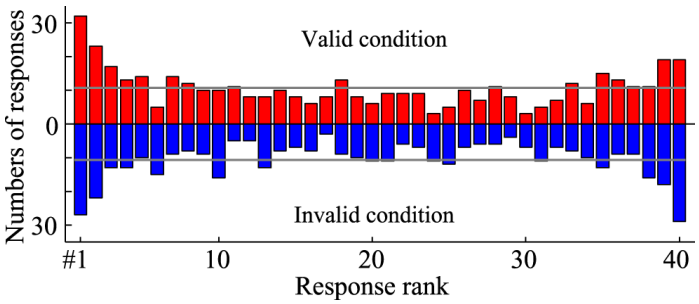

Figure 5 Distribution of the ranks of the responses to the target stimuli for the population of L-IPS neurons in the valid (red) and invalid (blue) conditions.
The rank of the response to each target stimulus was determined among the 40 responses of each neuron to the entire stimulus set. The histogram was then generated by counting the occurrences of each rank across the recorded L-IPS neurons. The height of the bars indicate the number of occurrences of each rank. The stimulus that induced the strongest response is ranked #1. Note that there were four different targets in each attention condition, so each neuron is counted four times to make the histogram. The gray line indicates the number of responses that would be expected if there is no bias in the distribution of the ranks.

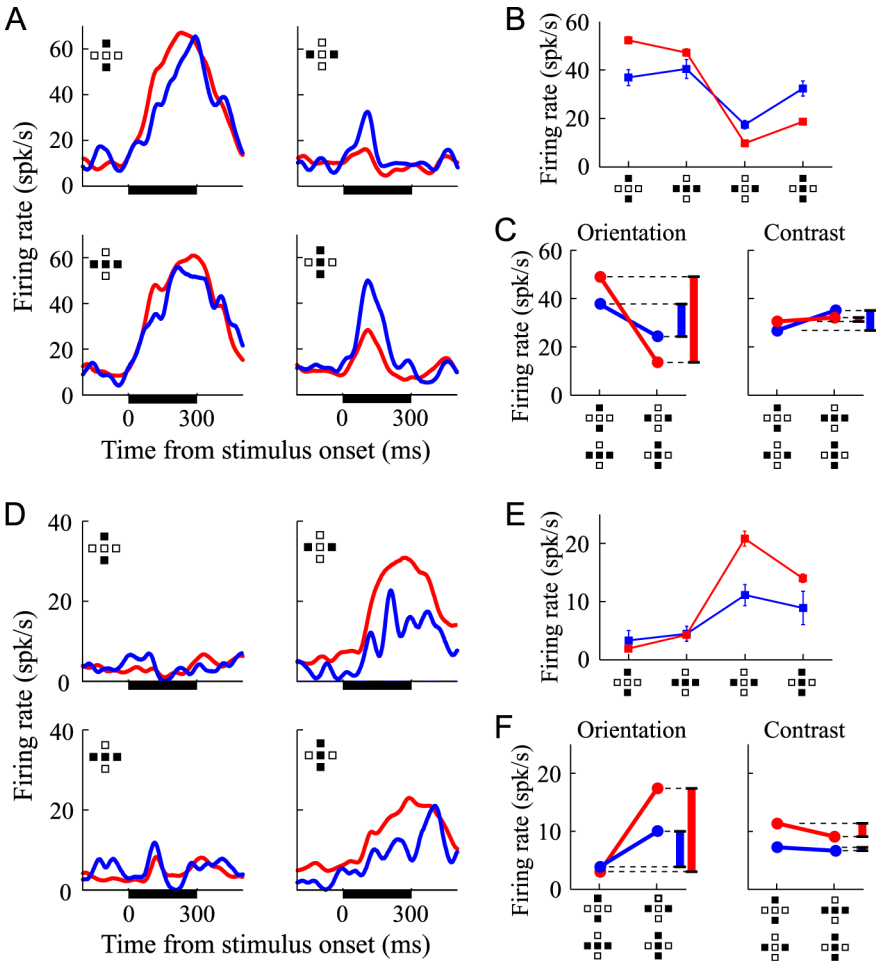

Figure 6 Responses of two representative L-IPS neurons to the target stimuli in the valid (red) and invalid (blue) conditions.
Panels A-C show responses of one neuron recorded from monkey GG, and panels D-F show the responses of a neuron from monkey FZ.
A: Spike density functions for the responses to the target stimulus illustrated in each panel.
B: Mean firing rate (with standard error of mean, SEM) of the response to each target stimulus.
C: Selectivity for the target orientation (left) and contrast (right). Each plot illustrates the average responses to the two target stimuli indicated below. The vertical bar on the right of each panel represents the difference between the responses that is dependent on the target orientations (DBO, left panel) and the difference that is dependent on the target contrast (DBC, right panel).
D-F: Shown using the same conventions as in A-C.

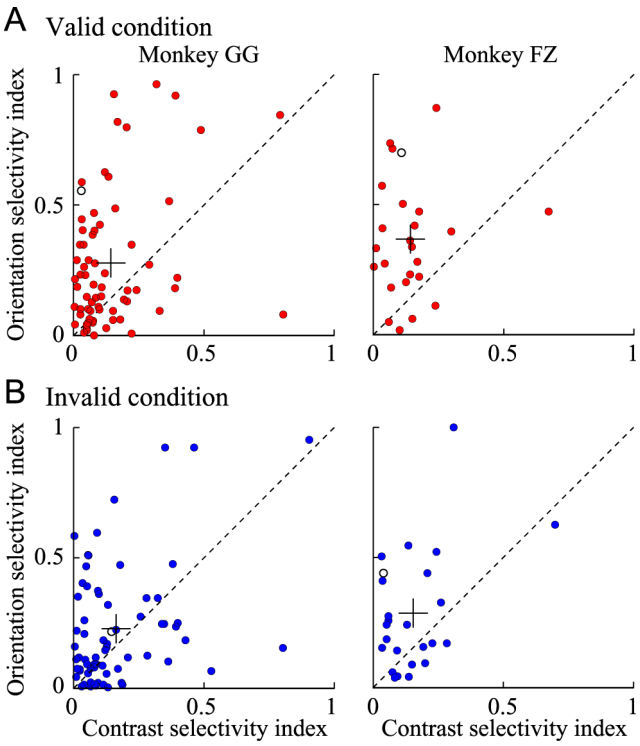

Figure 7 Comparison of the neuronal selectivities for target orientation and contrast across the population of recorded neurons.
A: Responses in the valid condition. Each point represents a neuron and is plotted at a position corresponding to its contrast selectivity index (horizontal axis) and the orientation selectivity index (vertical axis). Left and right panels show the data from monkeys GG and FZ, respectively. The cross indicates the average of the selectivity index. Open circles represent the result obtained with the neuron depicted in Fig. 6.
B: Responses in the invalid condition. Other conventions are the same as in A.

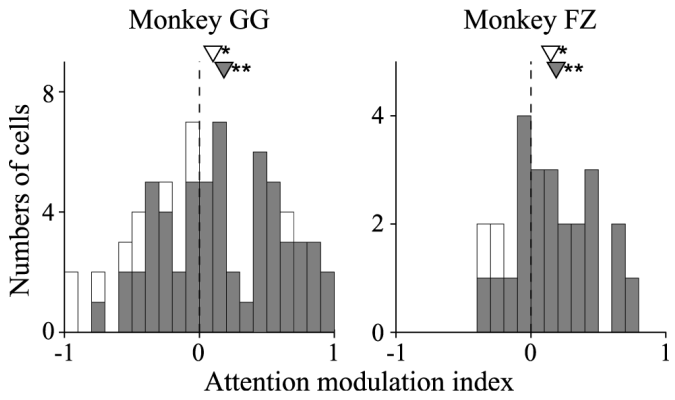

Figure 8 Distribution of the attention modulation index.
Left and right panels are for neurons recorded from monkeys GG and FZ, respectively. Open triangles indicate the average modulation indexes for the entire population. Dark gray bars represent neurons showing significant selectivity for the target orientation in ANOVA; the average modulation index for these neurons is indicated by a filled triangle. A positive value of the index indicates that the neuron exhibited greater selectivity in the valid condition than in the invalid condition. The asterisks denote statistical significance (*p < 0.05, **p < 0.01, *t* test).

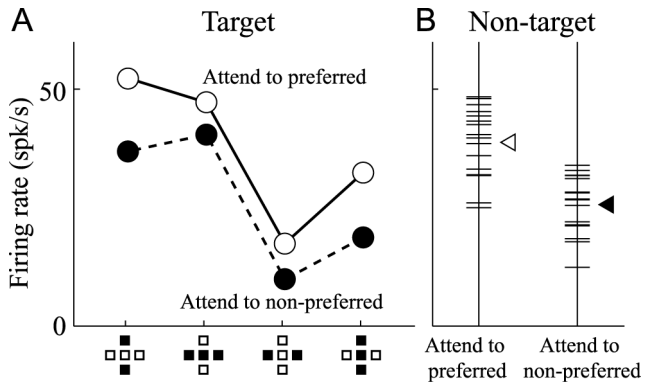

Figure 9 Effect of the attended orientation on the responses of an example neuron.
This is the same neuron depicted in Fig. 6A.
A: Responses to the target stimuli when the monkey directed its attention toward the preferred orientation (horizontal for this neuron, open circles) or toward the non-preferred orientation (vertical, filled circles).
B: Responses to the non-target stimuli when attention was directed toward the preferred orientation (left) and toward the non-preferred orientation (right). Short horizontal bars represent the responses to non-target stimuli. A triangle represents the mean.

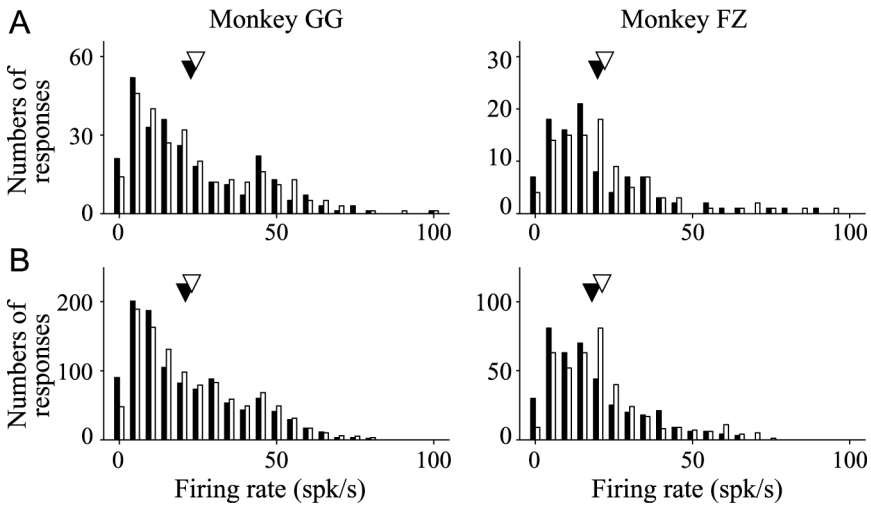

Figure 10 Effect of the attended orientation on the responses of the recorded neurons.
A: Responses of each neuron to the target stimuli when attention was directed toward its preferred (open bar) or non-preferred (filled bar) orientation. Triangles represent the mean responses in each condition. Left and right panels correspond to monkeys GG and FZ, respectively.
B: Responses to the non-target stimuli. Other conventions are the same as in A.
Note that each neuron provides four responses to the target stimuli and sixteen responses to the non-target stimuli in each attention condition.

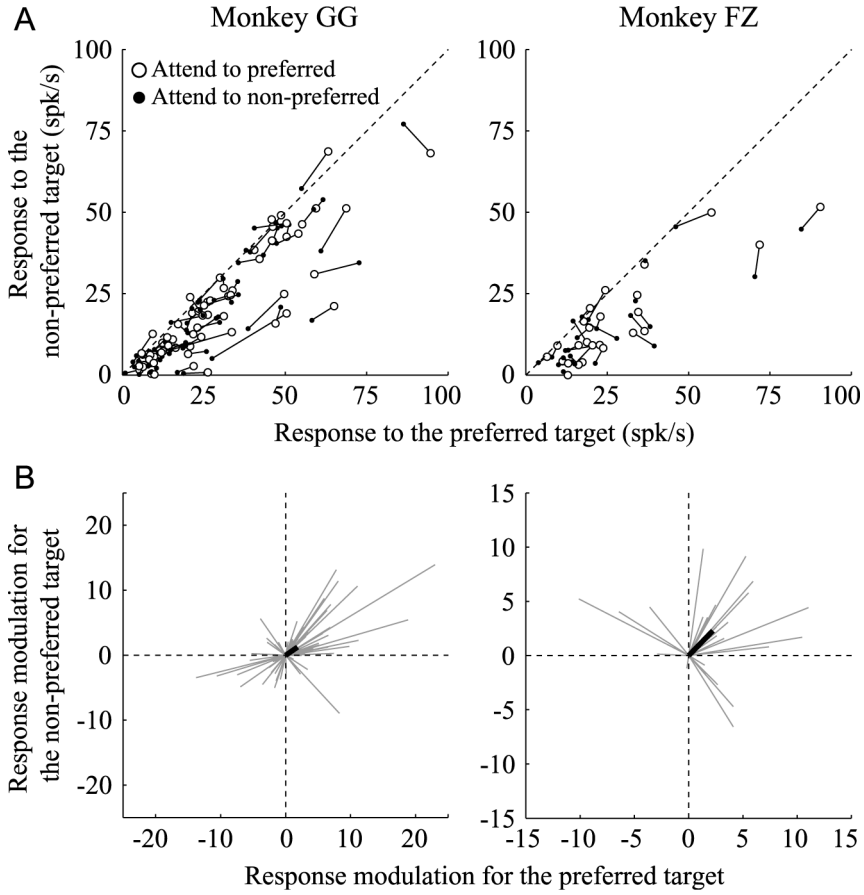

Figure 11 Comparison of the attentional modulation of responses to the target with the preferred orientation and to that with the non-preferred orientation.
A: Each data point represents the mean response of a single neuron to the target with the preferred orientation (horizontal axis) and to that with the non-preferred orientation (vertical axis). Open circles represent the response when the monkeys directed their attention toward the preferred orientation, and the filled circle when they directed it toward the non-preferred orientation. Data points obtained from the same neuron are connected by a line segment. Left and right panels correspond to monkeys GG and FZ, respectively.
B: Vector representation of the effects of attended orientation on the responses to the target. A thin-gray line represents as a vector the positional difference between the open and filled circles for each neuron in panel A. The origin of the coordinates corresponds to the response when the monkey directed its attention toward the non-preferred orientation and the end point of a vector corresponds to the response when it directed its attention toward the preferred orientation. A thick line indicates the average of the vectors. See text for details.

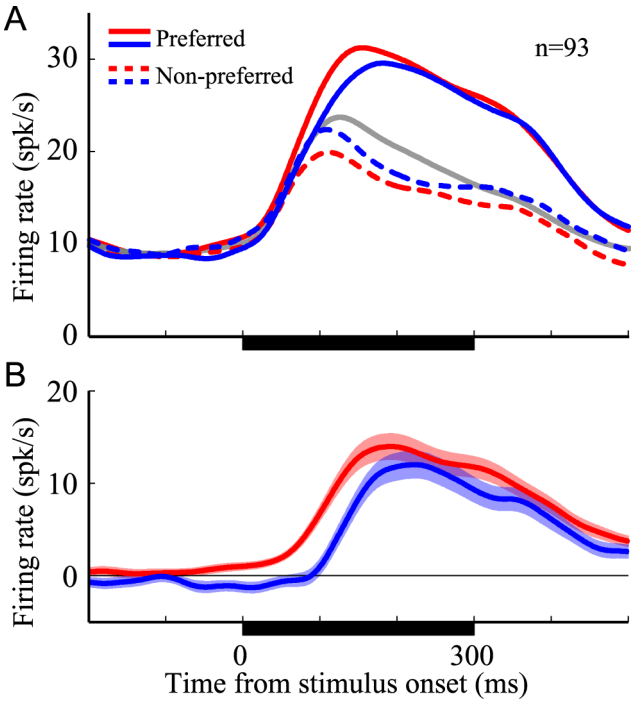

Figure 12 Time course of the visual responses in different conditions.
Averaged neuronal activities for the entire population (93 neurons) are shown for the valid (red) and invalid (blue) conditions.
A: Average responses to the target with the preferred orientation (solid line), the target with the non-preferred orientation (broken line), and non-target stimuli (gray line).
B: Average differences between the responses to the target with the preferred orientation and to that with the non-preferred orientation across the population of recorded neurons. Shaded area represents ±SEM.

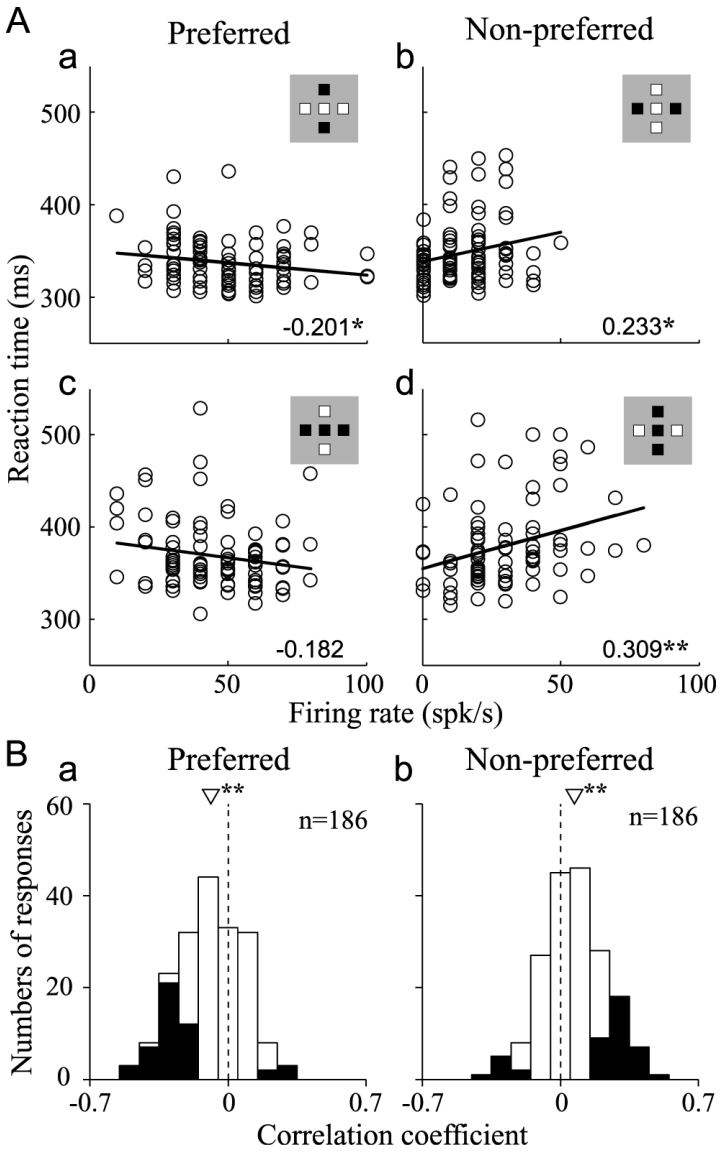

Figure 13 Correlation between neuronal activity and task performance.
A: Correlations between the magnitudes of the visual responses and the reaction times for the neuron depicted in Fig. 6A-C are shown. Each panel corresponds to the indicated target. For this neuron, horizontal is the preferred orientation (left column, a and c). In each panel, each data point reflects the mean firing rate computed in a trial (horizontal axis) and the reaction time in the same trial (vertical axis). The solid lines indicate the linear regression fits, and the numerical values indicate Pearson's correlation coefficient. The asterisks denote significance of the regression (*p < 0.05, **p < 0.01).
B: Correlation between neuronal activity and task performance for the population of recorded neurons. Distributions of the correlation coefficients computed for the responses to the target in the preferred (a) and non-preferred (b) orientations. The triangle indicates the average correlation coefficient. Note that the correlation was estimated for each target stimulus, so that each neuron provides two data points for each orientation. The asterisks denote significance of the regression (*p < 0.05, **p < 0.01, *t* test). Filled bars represent responses with significant correlation (p < 0.05).

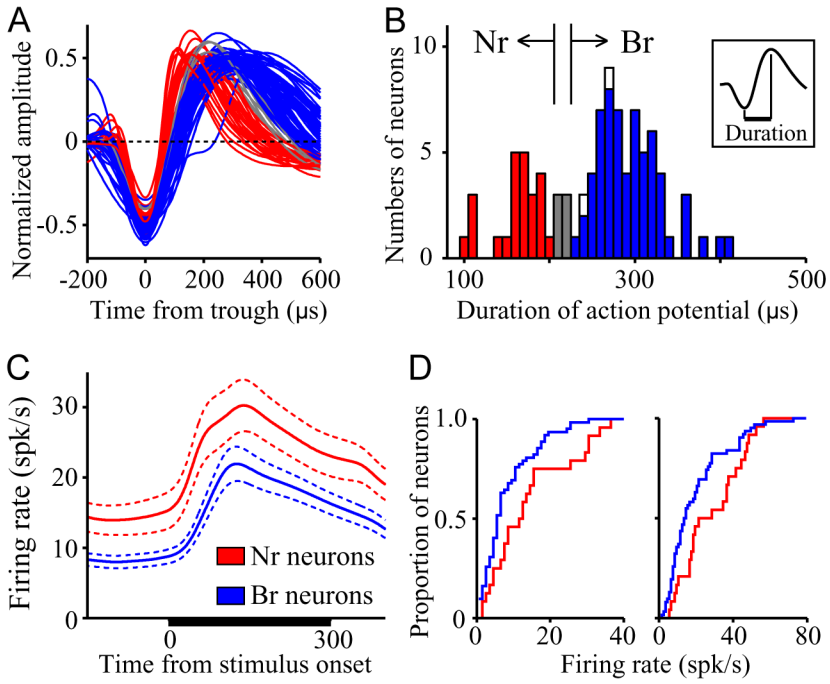

Figure 14 Classification of neurons according to action potential duration.
A: Averaged and normalized action potential for each of 94 neurons analyzed. Time was locked at the trough of each action potential.
B: Distribution of action potential durations. Based on the durations of their action potentials, neurons were classified as having a narrow action potential (Nr) or broad action potential (Br). Vertical lines indicate the criteria for classification. Six neurons around the criteria were excluded from analysis (gray, also shown in panel A). Two neurons switched the classification over recording session (white bars), and these were also excluded from analysis.
C: Averaged responses for each class of neurons under all stimulus conditions. The thick horizontal bar indicates the stimulus presentation period. Broken lines represent ±SEM.
D: Cumulative histogram for the firing rate during the epochs -150-0 ms before stimulus onset (left) and 50-250 ms after stimulus onset (right). Classified Br and Nr neurons are indicated by blue and red, respectively.

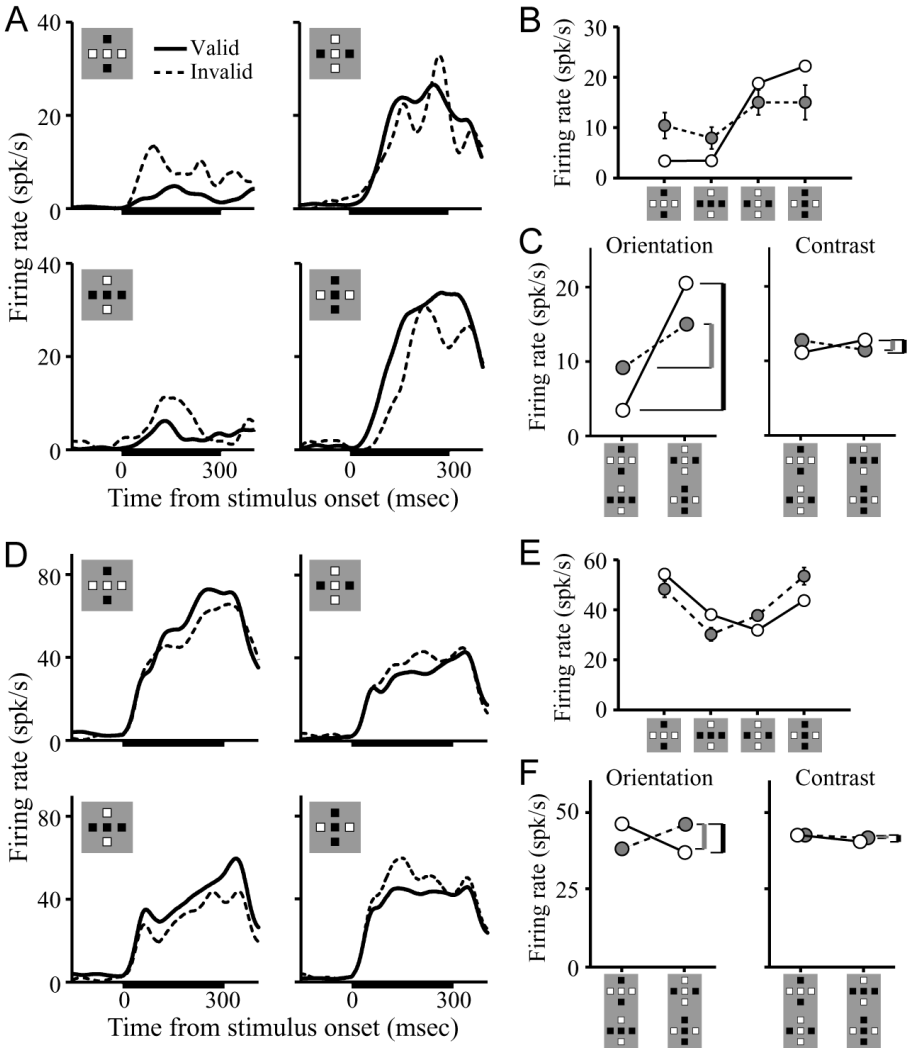

Figure 15 Responses of representative Br and Nr neurons to the target stimuli.
Neural activities are shown for the valid condition (black sold line and open symbols) and invalid condition (broken line and gray symbols). Panels A-C show responses of a Br neuron that showed orientation selectivity.
A: Spike density functions for the responses to the target stimulus illustrated in the inset in each panel. Spike density functions were obtained by convolving the spike train (1 ms resolution) with a Gaussian kernel (SD = 20 ms). The thick horizontal bars on the bottom indicate the stimulus presentation period.
B: Mean firing rate (with SEM) during the response to each target stimulus.
C: Selectivity for the target orientation (left) and contrast (right). Each plot illustrates the average responses to the two target stimuli indicated below. The vertical bars on the right of each panel represent differences between the responses that are dependent on the target orientations (DBO, left panel) or the target contrast (DBC, right panel).
Panels D-F show the responses of an example of Nr neuron, using the same conventions as panels A-C.

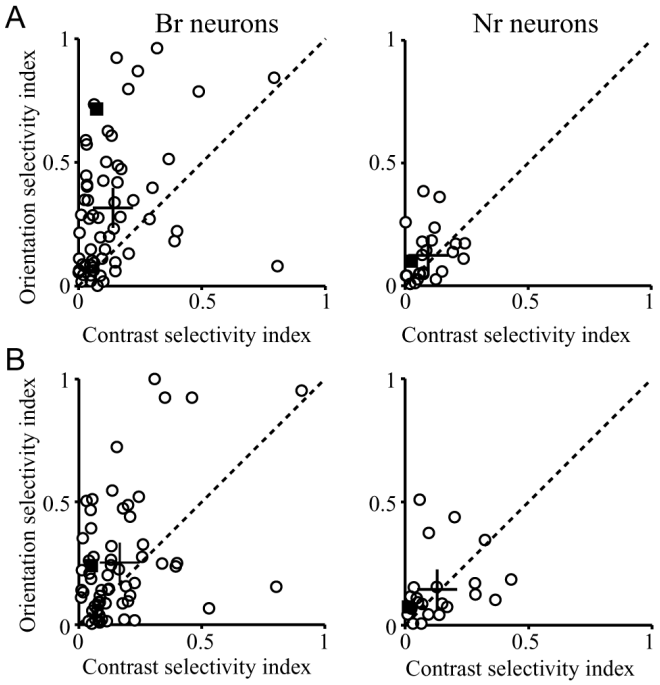

Figure 16 Comparison of the neuronal selectivities.
Left and right panels correspond to Br and Nr neurons, respectively.
A: Responses in the valid condition. Each point represents a neuron and is plotted at a position corresponding to its contrast selectivity index (horizontal axis) and orientation selectivity index (vertical axis). The cross indicates the average of the selectivity indexes.
B: Responses in the invalid condition. Conventions are the same as in A.
Filled squares in A and B show the result obtained with the neurons depicted in Fig. 15.

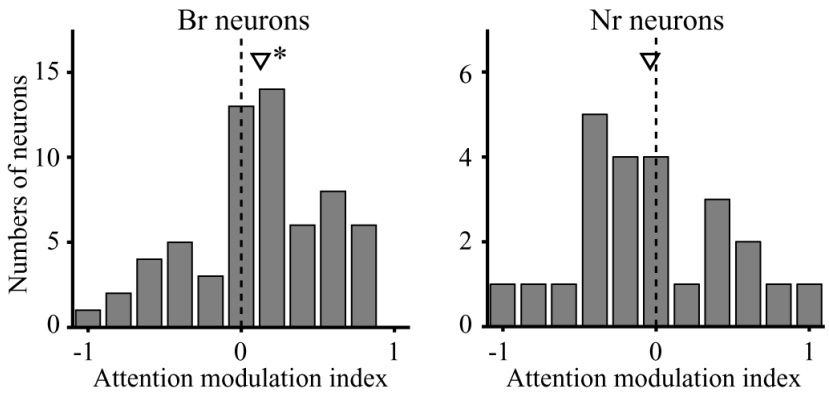

Figure 17 Distribution of the attentional modulation index.
Left and right panels correspond to Br and Nr neurons, respectively. Open triangles indicate the average modulation indexes for each population. A positive value of the index indicates that the neuron exhibited greater selectivity in the valid condition than the invalid condition. The asterisks denote statistical significance ($p < 0.05$, one sample Wilcoxon test).

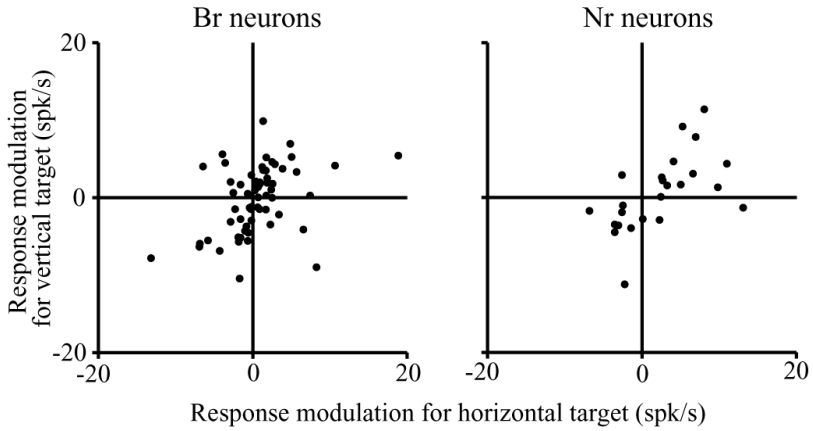

Figure 18 Comparison of the response modulation depending on the attended orientation for the responses to the horizontal target (horizontal axis) and that to the vertical target (vertical axis).
Each data point represents the response modulation of a single neuron, which was calculated by subtracting the average of the responses to the target when the monkey directed its attention toward the vertical orientation from that when the monkey directed its attention toward the horizontal orientation.

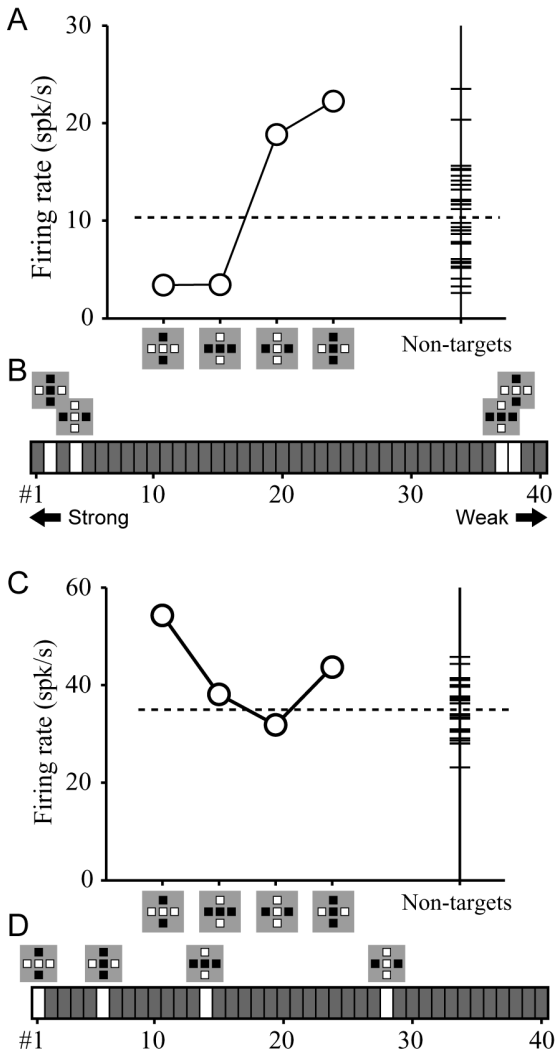

Figure 19 Comparison of responses to the target stimuli with those to the non-target stimuli.
A: Responses of the representative Br neuron depicted in Fig. 15A-C to targets and non-targets. The short horizontal lines to the right depict the magnitudes of the responses to each non-target stimulus, and the average of those responses is indicated by horizontal broken line.
B: Ranking of the responses to the target stimuli. There were 40 stimulus conditions: 4 targets and 16 non-targets presented in 2 attended orientations. Neuronal responses were sorted in order of response magnitude. White bars indicate the responses to the target stimuli in the valid condition.
Panels C and D shows the rank analysis of the responses of the Nr neuron depicted in Fig. 15D-F.

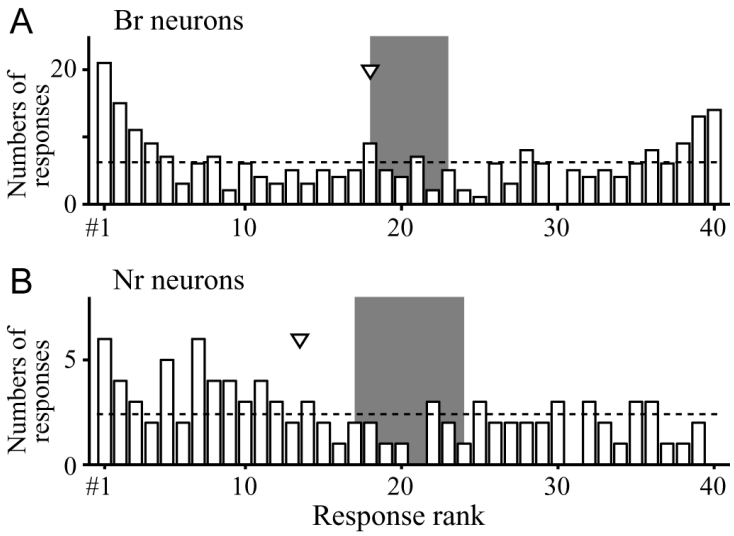

Figure 20 Distribution of the ranks of the responses to the target stimuli in the valid condition for the two classes of neurons.
The ranks of the responses to each target stimulus within the entire stimulus set were determined across the 40 responses of each neuron. A histogram was then generated by counting the occurrences of each rank across the recorded neurons. The height of the bars indicate the number of occurrences of each rank. The stimulus that induced the strongest response was ranked #1. Panels A and B depict the distributions of the ranks for Br and Nr neurons, respectively. A triangle indicates the median of the ranks for each population. The horizontal broken line indicates the number of responses that would be expected if there were no bias in the distribution of the ranks, and the gray area represents the 95% confidence interval for the median under that assumption computed using a permutation test. Note that there were four different targets, so each neuron was counted four times when making the histogram.

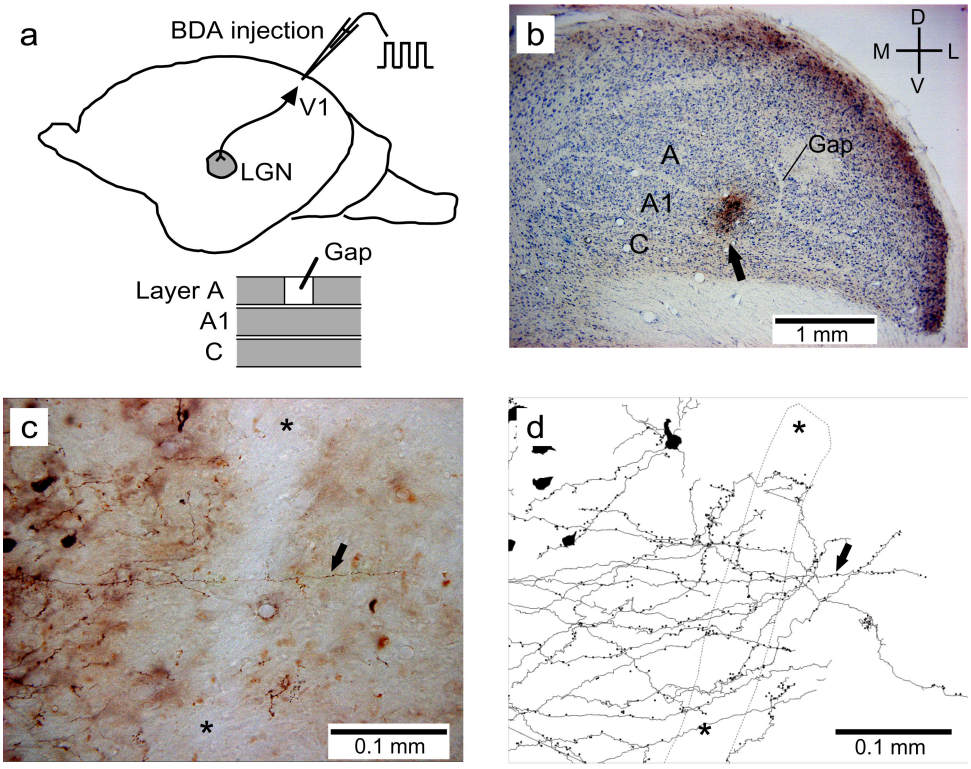

Figure 21 Feedback projection from V1 to the blind spot region of the LGN.
a: Schematic illustration of the experimental design (top) and the anatomical organization of the region in the LGN corresponding to the optic disk (bottom). The white square in layer A represents the neuron-free gap, which retinotopically corresponds to the optic disk.
b: Nissl-stained coronal section of the LGN showing the neuron-free gap corresponding to the optic disk. The black arrow indicates the dense patch of BDA-labeled axon terminals. The large neuron-free blob just above and lateral to the gap corresponds to the optic radiation that is formed by an upward curving of the posterior part of LGN (Sanderson 1971a). D: Dorsal, L: lateral: V: ventral, M: medial.
c: Magnified image of layer A around the neuron-free gap in a section without counter staining. An axon traversing the gap (arrow) can be seen. This photograph was taken by superimposing multifocal images.
d: Tracings of axons and boutons around the neuron-free gap made using Neurolucida. The dotted line marks the boundary of the gap. The black arrow indicates the axon shown in panel c. The region between the asterisks in panels c and d comprises the gap.